

Schematic Design of  
Distributed Mass Damping Systems  
for Tall Buildings

by

Jason Stahl Silbiger

Bachelor of Science in Civil Engineering  
University of Florida, 2013

Submitted to the Department of Civil and Environmental Engineering  
in Partial Fulfillment of the Requirements for the Degree of

MASTER OF ENGINEERING IN CIVIL AND ENVIRONMENTAL ENGINEERING

at the

MASSACHUSETTS INSTITUTE OF TECHNOLOGY

June 2014

©2014 Jason Stahl Silbiger. All Rights Reserved.

The author hereby grants to MIT permission to reproduce and to distribute publicly paper and electronic copies of this thesis document in whole or in part in any medium now known or hereafter created.

Signature of Author: \_\_\_\_\_

Department of Civil and Environmental Engineering  
May 9, 2014

Certified by: \_\_\_\_\_

Jerome J. Connor  
Professor of Civil and Environmental Engineering  
Thesis Supervisor

Certified by: \_\_\_\_\_

John A. Ochsendorf  
Professor of Building Technology and Civil and Environmental Engineering  
Thesis Supervisor

Accepted by: \_\_\_\_\_

Heidi M. Nepf  
Chair, Departmental Committee for Graduate Students



# Schematic Design of Distributed Mass Damping Systems for Tall Buildings

by

Jason Stahl Silbiger

Submitted to the Department of Civil and Environmental Engineering  
on May 9, 2014 in Partial Fulfillment of the  
Requirements for the Degree of Master of Engineering in  
Civil and Environmental Engineering

## ABSTRACT

As new high-rises grow taller and more slender, the design of tall buildings becomes heavily constrained by the control of lateral displacements and accelerations due to dynamic excitations. This has led to the development of motion control devices, such as the Tuned Mass Damper (TMD) and Tuned Liquid Column Damper (TLCD). Contemporary designs implement devices where the dynamic response is the greatest, often at the top of buildings, occupying entire floors and inhibiting the sale of valuable real estate. Conversely, distributed damping is the concept of dividing the dampers into smaller devices that are placed on several floors throughout the building. Although a greater total mass is required, implementing smaller dampers and using less valuable floor area may be advantageous for buildings with a substantial cost variation between floors.

This study presents a methodology where the optimal vertical distribution of TMDs and TLCDs is determined based on the footprint and relative cost of each damping scheme. To perform this analysis, the governing equations for a distributed damping system are developed and its response is derived assuming a periodic excitation.

Given the structural properties and performance requirements of the building, a one TMD system is designed using the conventional approach. Ranging through several distribution schemes, the damper mass required for each distribution to meet the same acceleration performance as the one TMD system is determined. This mass is used to calculate the damper footprint for TMD and TLCD systems. From the cost distribution of the building, the relative cost of each scheme may be calculated and compared. Depending on the objective of the designer, the minimum damper footprint or minimum cost scheme may be selected as the optimal distribution.

The methodology was demonstrated for 60, 80, 100, and 120-story buildings. It was observed that buildings with approximately half of the floors installed with dampers correspond to the minimum footprint scheme, while the minimum cost scheme was dependent on the building's size constraints and cost distribution. For buildings with significant cost variation in upper floors, distributed damping is not only the least cost solution, but also leads to conveniently small devices.

Thesis Supervisor: Jerome J. Connor

Title: Professor of Civil and Environmental Engineering

Thesis Supervisor: John A. Ochsendorf

Title: Professor of Building Technology and Civil and Environmental Engineering



## ACKNOWLEDGEMENTS

I would like to thank Dr. Connor for sharing with me his passion for structural engineering and introducing me to the topic of motion control.

Thank you to Dr. Ochsendorf for bringing me into the Structural Design Lab (SDL), providing a forum for innovative ideas, and always pushing my thesis on to the next question.

Daniel Gleave, Jonathan Ellowitz, Chelsea Sprague, and the rest of the SDL group have been instrumental in providing feedback on design assumptions and helping me consider the practical applications of distributed damping.

Thank you to Dr. Adams, Lauren McLean, and Kiley Clapper for running the Course 1 Master of Engineering program and always being available to help with our administrative needs.

Finally, to the 2014 M. Eng students for an incredible year of creative discussions, stress-relieving social activities, and long-lasting friendships.



## Table of Contents

Chapter 1: Introduction.....	13
Motion Control.....	13
Distributed Damping.....	14
Problem Statement.....	15
Chapter 2: Literature Review.....	17
TMD Development and Design.....	17
TLCD Development and Design.....	18
Distributed Damping Studies.....	21
Chapter 3: Distributed Damping Derivation.....	23
Governing Equations.....	23
Connectivity Matrix.....	24
Derivation.....	26
Chapter 4: Distribution Analysis.....	29
Simulation.....	29
Feasibility.....	30
Equivalent Performance.....	32
Chapter 5: Damper Footprint.....	35
TMD Footprint.....	35
TLCD Footprint.....	38
Chapter 6: Cost Analysis.....	43
Cost Curves.....	43
Optimal Scheme.....	46
Chapter 7: Conclusions.....	49
Discussion of Results.....	49

Future Research .....	50
Appendix A: Simulator .....	53
Appendix B: Damper Mass Iteration .....	57
Appendix C: TMD Footprint Calculation.....	61
Appendix D: TMD Footprint per Floor .....	63
Appendix E: TLCD Footprint Calculation .....	65
Appendix F: TLCD Footprint per Floor.....	67
Appendix G: Cost Calculation .....	69
Appendix H: Total Scheme Costs.....	71
Works Cited .....	75

## **List of Tables**

Table 4-1: Structural Properties .....	30
Table 4-2: Damper Properties for Feasibility Analysis .....	32
Table 5-1: Minimum TMD Footprint Schemes .....	37
Table 5-2: Minimum TLCD Footprint Schemes .....	40
Table 6-1: Optimal Schemes for All Buildings, Cost Curves, and Damping Systems.....	46
Table 6-2: Damper Dimensions of Optimal Scheme for 120 story Building .....	47



## List of Figures

Figure 1-1: Distributed Damping Methodology .....	15
Figure 2-1: SDOF-TMD Model.....	17
Figure 2-2: TLCD Model.....	19
Figure 3-1: nDOF-nTMD Model.....	23
Figure 3-2: 3DOF-2TMD Model.....	25
Figure 4-1: Acceleration Performance with Varying Distribution .....	31
Figure 4-2: Total Damper Mass Required to Meet 1TMD Performance.....	33
Figure 4-3: Percent Increase in Total Damper Mass Required to Meet 1TMD Performance .....	33
Figure 4-4: Mass Ratio Required to Meet 1TMD Performance .....	34
Figure 5-1: TMD Footprint per Floor for All Schemes in 60-story Building.....	37
Figure 5-2: Total TMD Footprint for All Schemes .....	38
Figure 5-3: TLCD Footprint per Floor for All Schemes in 60-story Building.....	40
Figure 5-4: Total TLCD Footprint for All Schemes.....	41
Figure 6-1: Cost Curves for 60-story Building.....	44
Figure 6-2: Total Scheme Costs for 60-story Building with Distributed TMDs .....	45
Figure 6-3: Total Scheme Costs for 60-story Building with Distributed TLCDs.....	45
Figure D-1: TMD Footprint per Floor for All Schemes in 80-story Building.....	63
Figure D-2: TMD Footprint per Floor for All Schemes in 100-story Building.....	63
Figure D-3: TMD Footprint per Floor for All Schemes in 120-story Building.....	64
Figure F-1: TLCD Footprint per Floor for All Schemes in 80-story Building.....	67
Figure F-2: TLCD Footprint per Floor for All Schemes in 100-story Building.....	67
Figure F-3: TLCD Footprint per Floor for All Schemes in 120-story Building.....	68
Figure H-1: Total Scheme Costs for 80-story Building with Distributed TMDs .....	71
Figure H-2: Total Scheme Costs for 80-story Building with Distributed TLCDs.....	71
Figure H-3: Total Scheme Costs for 100-story Building with Distributed TMDs .....	72
Figure H-4: Total Scheme Costs for 100-story Building with Distributed TLCDs.....	72
Figure H-5: Total Scheme Costs for 120-story Building with Distributed TMDs .....	73
Figure H-6: Total Scheme Costs for 120-story Building with Distributed TLCDs.....	73



## **Chapter 1: Introduction**

### **Motion Control**

Today's buildings are taller and more slender than ever. Unique challenges arise from new high-rises that aspire to be the signature structure of the area, while constrained by tight space limitations of cities. Additionally, these structures must resist extreme events such as hurricanes and earthquakes without occupant discomfort. Significant advancements in material strength and structural analysis have afforded contractors and engineers the tools to meet many of these challenges. However, while the strength of construction materials such as steel have roughly doubled over the past few decades, its stiffness has not significantly increased. This has led to a flexibility-based design approach where lateral deflections and accelerations are the dominant design constraints for tall buildings.

Another necessary design consideration for tall buildings is the dynamic response from earthquakes and vortex shedding. The light steel framing used in high-rise buildings has little inherent damping, or natural energy dissipation, and is vulnerable to dangerous and uncomfortable accelerations in near-resonant conditions. The dynamic amplification of these loading conditions may be reduced through either the redistribution of stiffness to avoid resonance or the implementation of damping in the building.

The need for motion control to meet serviceability requirements has led to the development of various energy dissipation methods and devices that are commonly used in contemporary design. Damping devices are either passive, which require no additional energy input, or they are active, which dampens the response with an input of energy usually through the implementation of actuators. Although there are many promising applications of active dampers, increased complexity, maintenance, and cost, and decreased reliability make passive dampers currently the more attractive option. Passive damping devices include hysteretic dampers, which dissipate energy through the cyclical inelastic deformation of materials, friction dampers, which are used to amplify the material interactions at connections, and viscous dampers, which incorporate a viscous fluid in a dashpot.

When these devices do not provide adequate energy dissipation, significant damping may be added to the structure through the use of a tuned mass damper (TMD). A TMD is an auxiliary

mass, usually on the order of two percent of the entire building mass, which is attached to the structure with springs and dashpots such that it is “tuned” to respond out of phase with the building. The inertial force of the mass dampens the response of the building. However, TMDs are mostly effective only when excited by the resonant frequency for which they are designed (usually the first or second mode). The design parameters include the mass of the TMD, which is selected based on the effective damping required and the feasibility of constructing and implementing the damper, the natural frequency of the TMD, which is selected to match the resonant frequency that is of concern, and the TMD damping, which causes a phase shift in the damper response. TMDs have many applications in buildings and bridges, and have been used in well-known high-rises such as the John Hancock Tower in Boston, the Citicorp tower in New York City, and Taipei 101 in Taiwan.

Another type of mass damping system is a relatively new device called a Tuned Liquid Column Damper (TLCD). A TLCD is a large U-shaped tube of water that flows back and forth with the structure and dissipates energy through fluid-surface interaction, the gravitational restoring force, transition effects at angles, and the head loss from orifices placed within the horizontal portion of the damper. TLCDs are advantageous due to their simplicity, low maintenance, and the ability to incorporate its water into emergency fire protection. The first high-rise implementation of the TLCD concept was used in the design of One Wall Centre in Vancouver.

### **Distributed Damping**

While TMDs and TLCDs are effective motion control devices, they are very large and most effective when placed near the top of the structure (for the first mode), which is the most valuable location of the building. Furthermore, TLCDs are limited in tall buildings by their space requirements due to the large stems necessary for long periods and TMDs require almost entire floors to allow for damper displacement. The distributed damping concept helps to meet these design constraints and to reduce the size of the dampers by dividing up the devices into smaller units that may be placed on several floors throughout the building.

However, there is a penalty for placing the dampers out of their most effective position. For the same performance as the contemporary one TMD scheme, the sum of the individual distributed masses must be greater than the mass necessary for one TMD. For buildings with a

significant cost difference between the lower and upper floors, the use of a distributed damping system may be advantageous.

### Problem Statement

This thesis presents a methodology for determining the optimal distributed placement of TMDs and TLCDs based on the performance requirements and cost distribution of a given building. A visual representation of the design methodology is presented in Figure 1-1. The building dimensions, mass, stiffness, and inherent damping are determined or specified based on the traditional design approach. Dependent on the additional damping required to meet acceleration constraints, the mass required for a one TMD scheme is calculated. Then, through an iterative process, the mass required for various distribution schemes ranging from two mass dampers to a damper on every floor is calculated. Each distribution scheme has a total footprint associated with it and is determined based on the density of the damping material or the space required to match the natural frequency of the specified resonant condition. Finally, a cost distribution is developed that expresses the variation of the cost per square meter depending on the vertical location in the building. Through application of the cost curve to each footprint, a total cost for each distribution scheme is calculated and the minimum cost, or optimal, scheme is selected.

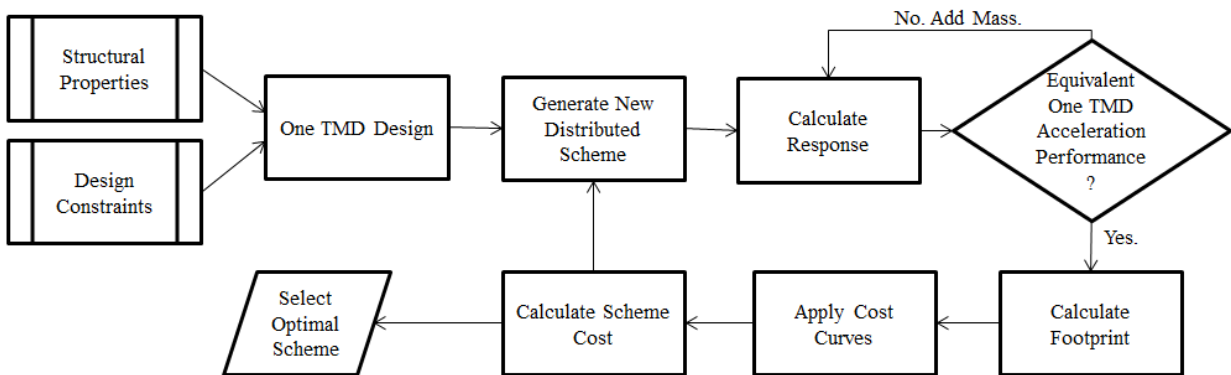


**Figure 1-1: Distributed Damping Methodology**

Through use of this methodology, developers and engineers can use known quantities such as the structural properties and cost distribution to determine the most cost-effective damping distribution with equivalent performance of the contemporary one TMD design scheme.

A review of the development and design of these damping systems are presented in Chapter 2. The governing equations for distributed mass damping systems and derivations for the simulation of structural response are developed and presented in Chapter 3. A distribution analysis is performed in Chapter 4 to determine the feasibility of distributed damping in tall buildings. Chapter 5 develops a procedure for estimating the damper footprint for each scheme and Chapter 6 applies cost curves to the footprints to determine an optimal distribution. Chapter 7 includes a discussion of the results and its value in contemporary design and construction processes.

## Chapter 2: Literature Review

### TMD Development and Design

The TMD concept was first applied by Frahm (1911) as a method to control ship vibrations and as an anti-rolling device. Den Hartog (1956) then developed a design methodology for mechanical applications where optimal parameters, such as the TMD damping ratio and the ratio of the damper's natural frequency to the structure's natural frequency, could be found to reduce the response. Tsai & Lin (1993) then performed empirical curve fitting techniques to calculate these optimal values for structures with inherent damping. Many experimental and numerical studies have been performed to apply the TMD methodology to multi-degree of freedom systems and to increase effectiveness. An example of the developments of this methodology includes the concept of Multiple Tuned Mass Dampers (MTMD). Igusa & Xu (1994) found that by placing TMDs next to each other with a variation of natural frequencies, the robustness could be increased. However, this scheme has a significant space requirement.

A single degree of freedom (SDOF), one TMD system is illustrated in Figure 2-1. Since TMDs are most effective for periodic loading rather than random excitations from earthquakes, a dynamic wind loading,  $p$ , is used to represent vortex shedding.  $m$ ,  $k$ , and  $c$  represent the mass, stiffness, and damping of the structure, respectively, while  $m_d$ ,  $k_d$ , and  $c_d$  represent the properties of the damper.

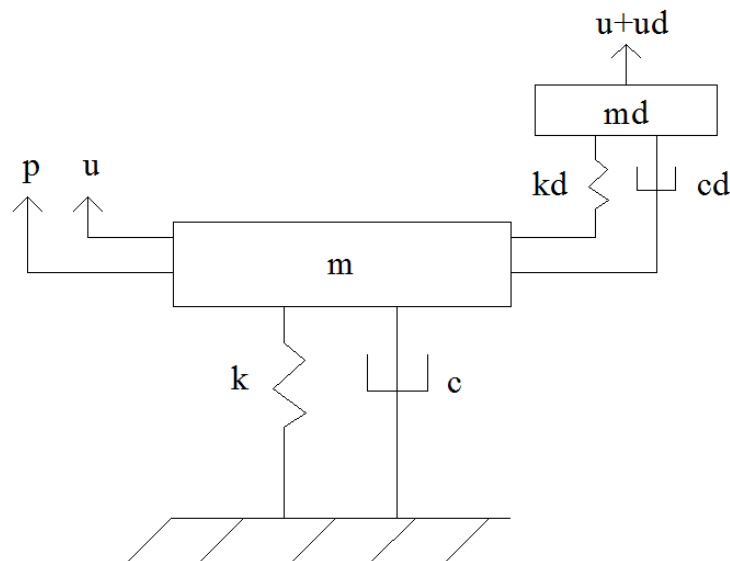


Figure 2-1: SDOF-TMD Model

The governing equations for this system are as follows:

Primary mass:

$$(m + m_d)\ddot{u} + c\dot{u} + ku = p - m_d\ddot{u}_d \quad (\text{Eqn. 2-1})$$

Damper:

$$m_d\ddot{u}_d + c_d\dot{u}_d + k_d u_d = -m_d\ddot{u} \quad (\text{Eqn. 2-2})$$

The first step in TMD design is to select a mass ratio ( $\bar{m}$ ) that provides the desired equivalent structural damping. Then, using charts and equations developed previously by Den Hartog and Tsai & Lin or through numerical optimization, an optimal damping ratio ( $\xi_{d|opt}$ ) and frequency ratio ( $f_{opt}$ ) is determined. With these quantities, the TMD properties can be calculated using the equations below. (Connor & Laflamme, 2014)

$$m_d = \bar{m} m \quad (\text{Eqn. 2-3})$$

$$k_d = \bar{m} f_{opt}^2 k \quad (\text{Eqn. 2-4})$$

$$\omega_d = \sqrt{\frac{k_d}{m_d}} \quad (\text{Eqn. 2-5})$$

$$c_d = 2\xi_{d|opt} \omega_d m_d \quad (\text{Eqn. 2-6})$$

For multi degree of freedom (MDOF) systems, the above equations may be used with the mass and stiffness of the structure replaced by the modal mass ( $\tilde{m}$ ) and modal stiffness ( $\tilde{k}$ ). Otherwise, the design procedure is equivalent.

## TLCD Development and Design

Sakai (1989) invented the TLCD as a new type of vibration absorber for buildings and developed the equations that govern the response. Through numerical simulation, Xu (1992) found that the TLCD system could provide the same level of effectiveness as the TMD. To increase the damping of the TLCD, an orifice is added to the horizontal section of the U-tube, which introduces an additional head loss to the fluid. Many parametric studies have been performed regarding these orifice ratios (Samali, Kwok, & Tapner, 1992; Samali, Mayol, Kwok, Hitchcock, & Wood, 2002; Colwell & Basu, 2006). It has also been experimentally demonstrated

that TLCDs can perform adequately regardless of the principle axis of excitation when using a bidirectional TLCD (Hitchcock, Kwok, Watkins, & Samali, 1997). Similar to the MTMD concept, multiple TLCDs tuned to varying frequencies have been shown to be less sensitive to frequency ratio but are limited by their high liquid motion (Gao, Kwok, & Samali, 1999). Over the past couple of decades, numerous studies have been conducted to modify the TLCD to increase effectiveness. These include, adjusting the ratio of the column area to the horizontal area (Hitchcock, Kwok, Watkins, & Samali, 1997), using a V-shaped horizontal section for strong excitations (Gao, Kwok, & Samali, 1997), and experimenting with viscous fluids (Colwell & Basu, 2008). Additionally, the applications of TLCDs to varying structures and excitations such as tapered buildings (Balendra, Wang, & Rakesh, 1998) and earthquakes (Mayol, Samali, Kwok, & Li, 2003) have been studied concluding adequate TLCD effectiveness.

As shown in Figure 2-2, the governing equations for the TLCD are developed from the drag force ( $F_d$ ) of the liquid and the friction force ( $F$ ) that acts at the interface of the TLCD and the primary mass. These forces have been calculated by Connor & Laflamme (2014) using conservation of energy principles.

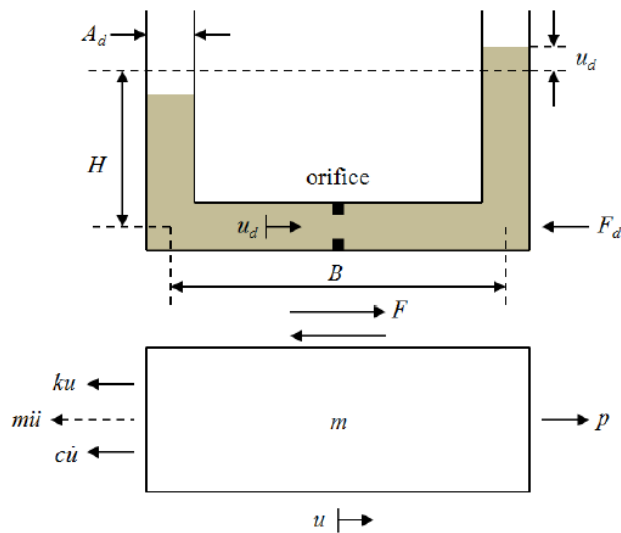


**Figure 2-2: TLCD Model (Adapted from Connor & Laflamme, 2014)**

Substituting  $F$  and  $F_d$  into the equations of motion for this system, lead to the following governing equations:

Primary mass:

$$m\ddot{u} + c\dot{u} + ku + \rho'A_d(B + 2H)\ddot{u} + \rho'A_dB\ddot{u}_d = p \quad (\text{Eqn. 2-7})$$

Damper:

$$F_d = - [\rho'A_dB\ddot{u} + \rho'A_d(B + 2H)\ddot{u}_d + \alpha\rho'gA_du_d] \quad (\text{Eqn. 2-8})$$

Where  $\rho'$  is defined as the fluid density,  $B$  is the damper width,  $H$  is the stem height,  $A_d$  is the damper cross-sectional area, and  $\alpha$  is a geometric constant.

Defining  $L_d$  as the total damper length ( $B + 2H$ ),  $\beta$  as the ratio of the width to the total length ( $B/L_d$ ), and equating the following damping properties:

$$m_d = \rho'A_dL_d \quad (\text{Eqn. 2-9})$$

$$k_d = \alpha\rho'A_dg \quad (\text{Eqn. 2-10})$$

where  $\alpha = 1$ , if  $\beta = 1$  and  $\alpha = 2$ , if  $\beta < 1$

$$F_d = c_{eq}\dot{u}_d \quad (\text{Eqn. 2-11})$$

Eqn. 2-7 and 2-8 become

Primary mass:

$$(m + m_d)\ddot{u} + c\dot{u} + ku = p - \beta m_d\ddot{u}_d \quad (\text{Eqn. 2-12})$$

Damper:

$$m_d\ddot{u}_d + c_{eq}\dot{u}_d + k_du_d = -\beta m_d\ddot{u} \quad (\text{Eqn. 2-13})$$

Since the fluid damping in the TLCD is nonlinear, an equivalent viscous damping constant ( $c_{eq}$ ) is used in this formulation and calculated by equating the energy dissipation (through hysteretic loops) of the TLCD to a viscous damper. Notably, after making these substitutions, the governing equations of the TMD (Eqn. 2-1 and 2-2) and the TLCD (Eqn. 2-12 and 2-13) are identical except for the  $\beta$  term. Furthermore, example calculations from Connor & Laflamme (2014) have shown that the TLCD is most effective when  $\beta = 1$ , when the fluid rests

only in the horizontal portion of the TLCD in the steady state. For this study, TLCDs will be designed under this condition and therefore the TMD governing equations and design procedure will be used for both mass damping systems.

### **Distributed Damping Studies**

The concept of placing TMDs throughout a structure has not been extensively studied. Bergman (1989), through numerical studies of a cantilever beam model, concluded that by placing TMDs throughout the upper floors of a building, there is not a significant loss of effectiveness. Chen (1996, 2001) later applied this concept to a 6-story building model to study the effectiveness of TMDs subjected to seismic excitations. He found that by dividing up the mass of the TMDs, the overstroke effect - in-phase movement of TMDs that increase structural response - would be reduced, since the inertial force of each TMD is less. Moon (2005, 2010, 2011) used MTMDs and distributed TMDs as part of his double skin façade study to integrate motion control within the exterior walls of the structure. He concluded that distributed damping for tall buildings is feasible and performed a 60-story design example where the distribution scheme was an initial design decision.

While this paper draws on the distributed damping models in previous studies, the derivations and methodology presented hereafter are applied where the distribution of damper mass is a result of the design rather than a decision. Furthermore, the methodology is extended to include varying building heights and both TMD and TLCD systems.



## Chapter 3: Distributed Damping Derivation

### Governing Equations

In order to simulate the response of a structure with a distributed mass damping system, the governing equations are developed for an n-degree of freedom structure (nDOF) with an n-number of TMDs. A model of this generalized system is presented in Figure 3-1.

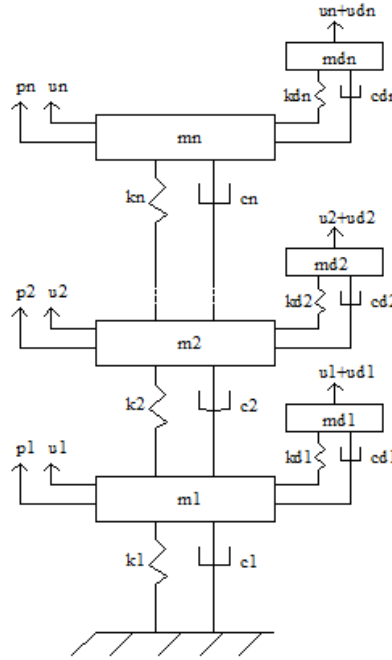


**Figure 3-1: nDOF-nTMD Model (Adapted from Moon, 2005)**

Performing equilibrium at each node and each damper lead to the following equations of motion:

Primary mass:

$$\bar{m}\ddot{u} + \bar{c}\dot{u} + \bar{k}u = \bar{p} + \bar{k}_d u_d + \bar{c}_d \dot{u}_d \quad (\text{Eqn. 3-1})$$

Damper:

$$\bar{m}_d \ddot{u}_d + \bar{c}_d \dot{u}_d + \bar{k}_d u_d = -\bar{m}_d \ddot{u} \quad (\text{Eqn. 3-2})$$

Combining Eqns. 3-1 and 3-2 lead to a more convenient form of the primary mass equation:

$$(\bar{m} + \bar{m}_d)\ddot{u} + \bar{c}\dot{u} + \bar{k}u = \bar{p} - \bar{m}_d\ddot{u}_d \quad (\text{Eqn. 3-3})$$

Eqns. 3-2 and 3-3 have the same form of the governing equations as the SDOF-TMD model shown earlier in Eqns. 2-1 and 2-2. Except, now, each distributed damping equation is comprised of a set of  $n$ -equations. Matrix notation is used to represent these coupled equations. Each structural property is related to its corresponding local matrix, as shown below.

$$\bar{m} = \begin{bmatrix} m_1 & 0 & 0 & 0 \\ 0 & m_2 & 0 & 0 \\ 0 & 0 & \ddots & 0 \\ 0 & 0 & 0 & m_n \end{bmatrix} \quad \bar{m}_d = \begin{bmatrix} m_{d1} & 0 & 0 & 0 \\ 0 & m_{d2} & 0 & 0 \\ 0 & 0 & \ddots & 0 \\ 0 & 0 & 0 & m_{dn} \end{bmatrix}$$

$$\bar{k} = \begin{bmatrix} k_1+k_2 & -k_2 & 0 & 0 \\ -k_2 & k_2+k_3 & \ddots & 0 \\ 0 & \ddots & \ddots & -k_n \\ 0 & 0 & -k_n & k_n \end{bmatrix} \quad \bar{k}_d = \begin{bmatrix} k_{d1} & 0 & 0 & 0 \\ 0 & k_{d2} & 0 & 0 \\ 0 & 0 & \ddots & 0 \\ 0 & 0 & 0 & k_{dn} \end{bmatrix}$$

$$\bar{c} = \begin{bmatrix} c_1+c_2 & -c_2 & 0 & 0 \\ -c_2 & c_2+c_3 & \ddots & 0 \\ 0 & \ddots & \ddots & -c_n \\ 0 & 0 & -c_n & c_n \end{bmatrix} \quad \bar{c}_d = \begin{bmatrix} c_{d1} & 0 & 0 & 0 \\ 0 & c_{d2} & 0 & 0 \\ 0 & 0 & \ddots & 0 \\ 0 & 0 & 0 & c_{dn} \end{bmatrix}$$

Additionally, each response and force is represented with an array.

$$u = \begin{bmatrix} u_1 \\ u_2 \\ \vdots \\ u_n \end{bmatrix} \quad u_d = \begin{bmatrix} u_{d1} \\ u_{d2} \\ \vdots \\ u_{dn} \end{bmatrix} \quad \bar{p} = \begin{bmatrix} p_1 \\ p_2 \\ \vdots \\ p_n \end{bmatrix}$$

The mass of the structure and the damping constants are comprised of diagonal matrices since their properties are not coupled with other nodes. However, the stiffness and damping of the structure is made up of tri-diagonal matrices where the values are coupled with their adjacent node's properties.

### Connectivity Matrix

For distributed damping schemes where there are not TMDs or TLCDs at every node, a connectivity matrix,  $\bar{E}$ , is introduced to modify the damper matrix equations and match the scheme to be analyzed. The connectivity matrix is of size  $n$ -by- $r$ , where  $n$  is the number of nodes

and  $r$  is number of dampers. Filled only with ones and zeroes, a one is placed in the row number corresponding to a node with a damper. There is only one value per row, since only one damper is placed at a given node for this analysis. Each column represents the damper number that is being assigned. For example, in the variable TMD scheme shown in Figure 3-2, where there are three nodes and only dampers attached to the top two, the connectivity matrix would be as follows:

$$\bar{E} = \begin{bmatrix} 0 & 0 \\ 1 & 0 \\ 0 & 1 \end{bmatrix}$$

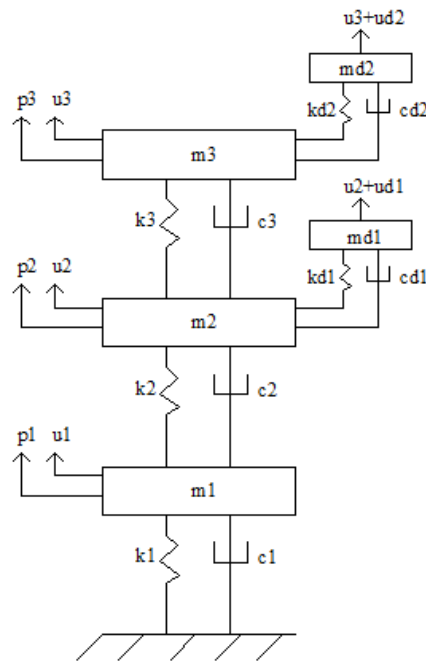


**Figure 3-2: 3DOF-2TMD Model**

The connectivity matrix is applied to the damper mass matrix, using the following expressions:

$$\bar{m}'_d = \bar{E}\bar{m}_d\bar{E}^T \quad (\text{Eqn. 3-4})$$

$$\bar{m}''_d = \bar{E}\bar{m}_d \quad (\text{Eqn. 3-5})$$

With this manipulation, the governing equations for a variable distributed damping scheme may be expressed as follows:

Primary mass:

$$(\bar{m} + \bar{m}'_d)\ddot{u} + \bar{c}\dot{u} + \bar{k}u = \bar{p} - \bar{m}''_d\ddot{u}_d \quad (\text{Eqn. 3-6})$$

Damper:

$$\bar{m}_d\ddot{u}_d + \bar{c}_d\dot{u}_d + \bar{k}_d u_d = -\bar{m}''_d{}^T \ddot{u} \quad (\text{Eqn. 3-7})$$

## Derivation

To solve the n-governing equations of the primary mass and the r-governing equations of the dampers simultaneously, Eqns. 3-6 and 3-7 are combined to form the following equation:

$$M\ddot{U} + C\dot{U} + KU = P - M^*U \quad (\text{Eqn. 3-8})$$

where the above global matrices are defined as:

$$M = \begin{bmatrix} \bar{m} + \bar{m}'_d & 0 \\ 0 & \bar{m}_d \end{bmatrix} \quad K = \begin{bmatrix} \bar{k} & 0 \\ 0 & \bar{k}_d \end{bmatrix} \quad C = \begin{bmatrix} \bar{c} & 0 \\ 0 & \bar{c}_d \end{bmatrix} \quad M^* = \begin{bmatrix} 0 & \bar{m}''_d \\ \bar{m}''_d{}^T & 0 \end{bmatrix}$$

$$U = \begin{bmatrix} u \\ u_d \end{bmatrix} \quad P = \begin{bmatrix} \bar{p} \\ 0 \end{bmatrix}$$

Now that a single equation has been developed that governs the response of the system, steps may be taken to solve the differential equation for the displacement vector,  $U$ . Since the damping systems investigated in this study are more effective for vortex shedding, rather than seismic excitation, the loading scenario in this derivation is assumed to be periodic. As with periodic excitations, it is convenient to work in the frequency domain and with complex quantities. Therefore, the loading is defined as:

$$P = \hat{P}e^{i\Omega t} \quad (\text{Eqn. 3-9})$$

where  $\hat{P}$  is the magnitude of the load and  $\Omega$  is the forcing frequency.

It follows that the response is also assumed to be periodic and may be differentiated to form the following equations:

$$U = \hat{U}e^{i\Omega t} \quad (\text{Eqn. 3-10})$$

$$\dot{U} = i\Omega\hat{U}e^{i\Omega t} \quad (\text{Eqn. 3-11})$$

$$\ddot{U} = -\Omega^2 \hat{U} e^{i\Omega t} \quad (\text{Eqn. 3-12})$$

where  $\hat{U}$  denotes the magnitude of the response.

Substituting Eqns. 3-9 through 3-12 into the governing equation and cancelling out the time varying terms, Eqn. 3-8 becomes:

$$-M\Omega^2 \hat{U} + iC\Omega \hat{U} + K\hat{U} = P - M^* \Omega^2 \hat{U} \quad (\text{Eqn. 3-13})$$

By collecting terms, isolating  $\hat{U}$ , and taking the absolute value of the complex quantity, the magnitude of the displacement vector is solved as:

$$\hat{U} = \left\| \left[ K - (M + M^*)\Omega^2 + iC\Omega \right]^{-1} P \right\| \quad (\text{Eqn. 3-14})$$

Furthermore, the magnitude of the acceleration vector can be solved using the relationship in Eqn. 3-12, now expressed as:

$$\hat{\ddot{U}} = \Omega^2 \hat{U} \quad (\text{Eqn. 3-15})$$

With Eqns. 3-14 and 3-15, the response of any distributed damping scheme may be solved by populating the local matrices with the system properties and loading conditions, and simply performing linear algebra.



## Chapter 4: Distribution Analysis

### Simulation

From the derivations in Chapter 3, a simulator has been created where the structural properties of the building and number of dampers are specified, and the program designs the damper parameters and calculates the response. The MATLAB code for this procedure can be found in Appendix A. The distribution schemes considered in this study are a 1TMD system (the conventional design) through an nTMD system (a damper placed at every floor). The dampers are distributed on consecutive floors, starting at the top of the building. For example, a two damper scheme is modeled with a damper located on each of the top two floors, while a nine damper scheme has a damper at each of the top nine floors.

To present the feasibility of this concept and demonstrate the methodology, 60, 80, 100, and 120-story buildings are used as design examples in this study. Simplifying assumptions were made in the selection of the structural properties for ease of analysis and computation, as it is the relative performance of the damping schemes rather than the absolute response of the structure that is studied. The mass and stiffness of each floor is assumed to be constant and inherent damping is assumed to be negligible in order to more clearly see the effect of the motion control devices. Once the mass is estimated, the stiffness is iterated so that the maximum deflection with motion control would not exceed  $1/400^{\text{th}}$  of the total height. The building dimensions were calculated assuming a square footprint, a 1:7 (base:height) slenderness ratio, and a floor height of 4.4 meters. A more detailed list of the structural properties, including building dimensions, floor mass ( $m$ ), interstory stiffness ( $k$ ), damping ( $c$ ), and natural frequency ( $\omega$ ) is shown in Table 4-1.

This analysis considers the worst-case loading scenario, a resonant condition where the forcing frequency is equal to the first natural frequency of the structure. This assumption is made to be conservative and to consider a loading where the dampers are excited in the response. The wind loading is assumed to be a uniform 1500 Pascals, resolved at each node using a tributary analysis.

For ease of construction and design, the dampers in this study are assumed to be modular, where the mass, stiffness, and damping are all constant. The frequency and damping ratios used to find TMD and TLCD properties are calculated using Den Hartog's (1956) formulae discussed

in Chapter 2. However, for actual optimal parameters, a numerical optimization technique is necessary for each distribution scheme and is beyond the scope of this study. Finally, the mass ratio, which in practice would be determined based on the acceleration constraint and the feasibility of construction, is selected to be the typical value of 2%.

**Table 4-1: Structural Properties**

Floors	Height (m)	Width (m)	m (Mg)	k (GN/m)	c (Ns/m)	$\omega$ (rad/s)
60	264	37.7	2500	6.3	0	0.117
80	352	50.3	2500	11.1	0	0.166
100	440	62.9	2500	17.4	0	0.262
120	528	75.4	2500	25.0	0	0.436

### Feasibility

Since the distribution concept places dampers out of their most effective location, it is important to analyze and evaluate to what extent the distribution of each scheme affects the structural performance. The following analysis uses the maximum acceleration of the structure as the representative response parameter and compares it to the 1TMD conventional design scheme. The damper mass of the 1TMD scheme is used as the sum of all damper masses for each scheme. For example, in the 2TMD scheme, each damper has 50% of the mass of the damper in the 1TMD scheme; the 3TMD scheme has a damper mass that is 33% of the 1TMD scheme, and so on. This is specified so that the total damper mass is equivalent for all distributions in this analysis and a reasonable comparison can be made. Figure 4-1 shows the percent increase in maximum acceleration for each distribution compared to the 1TMD scheme. The analysis is performed for all four buildings.

The acceleration data grow parabolically as the number of dampers in the scheme increase, but do so at a lower rate for taller buildings. A shallow slope in the acceleration curves represents a minimal loss in performance as more dampers are added to the scheme, while a steep slope represents a large loss in performance. Therefore, there is only a small decrease in performance as the first few dampers are added, but once the majority of the floors has dampers, additional devices do not significantly participate in the response and the performance decreases drastically. However, for tall buildings, there is a substantial amount of dampers that may be added before the performance significantly diminishes. For example, if a 5% increase in

response was tolerable for the structures in this analysis, a distributed scheme with as many as 15 dampers for the 60-story building and 30 for the 120-story building would be applicable using the same total damper mass. Since, under this scenario, similar performance can be maintained with individual dampers that have 6.7% (60-story) to 3.3% (120-story) of the mass of the conventional scheme, there may be substantial cost benefits in implementing the smaller devices and redistributing the damper footprint to lower floors. The damper properties for this analysis, including the mass ( $m_d$ ), stiffness ( $k_d$ ), and damping ( $c_d$ ) for the conventional design and the scheme where there is a 5% increase in response ( $A_{max}$ ) are presented in Table 4-2. Notably, these damper design values for the distributed schemes are the same regardless of building height. It is only the number of dampers that vary. However, with numerically optimized frequency and damping ratios for each scheme, this may no longer be the case.

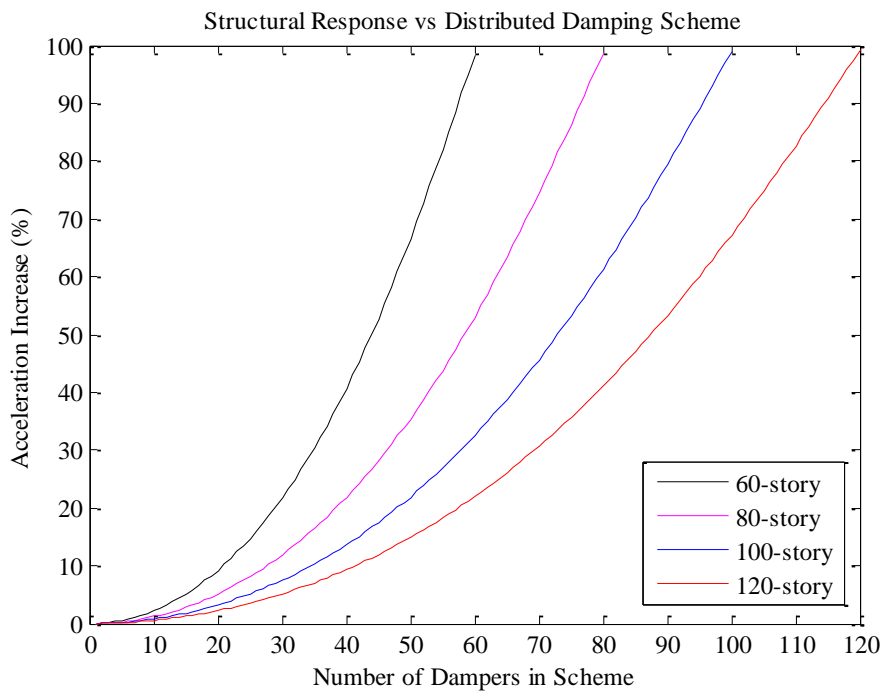


**Figure 4-1: Acceleration Performance with Varying Distribution**

**Table 4-2: Damper Properties for Feasibility Analysis**

	Floors	Dampers	$m_d$ (Mg)	$k_d$ (kN/m)	$c_d$ (kNs/m)
1TMD Scheme	60	1	1510	2430	325
	80	1	2010	3250	433
	100	1	2510	4070	542
	120	1	3010	4880	650
5% $A_{max}$ increase	60	15	101	162	21.7
	80	20	101	162	21.7
	100	25	101	162	21.7
	120	30	101	162	21.7

### Equivalent Performance

The next step is to find the damper mass required for each scheme and each building, where no loss in structural performance compared to the conventional design is achieved. With equivalent performing schemes, direct comparisons can be made of the footprint and cost for each distribution (discussed in Chapters 5 and 6). The procedure involves designing a 1TMD system and recording the maximum acceleration of the structure. This response parameter is used as the threshold performance value necessary for all schemes. Then, for each distribution, iteration through the damper mass is run until the acceleration response meets the design constraint previously found. The MATLAB code executing this procedure is presented in Appendix B. Figure 4-2 shows the total mass required for equivalent performance for each scheme and building. This result divided by the number of dampers is the raw data used to determine the damper footprint. Figure 4-3 illustrates how the mass required increases as a percentage of the 1TMD scheme, while Figure 4-4 displays the mass ratio necessary for each distribution. In practice, these plots may be used early in the design process as an additional consideration when selecting a mass ratio for the motion control system.

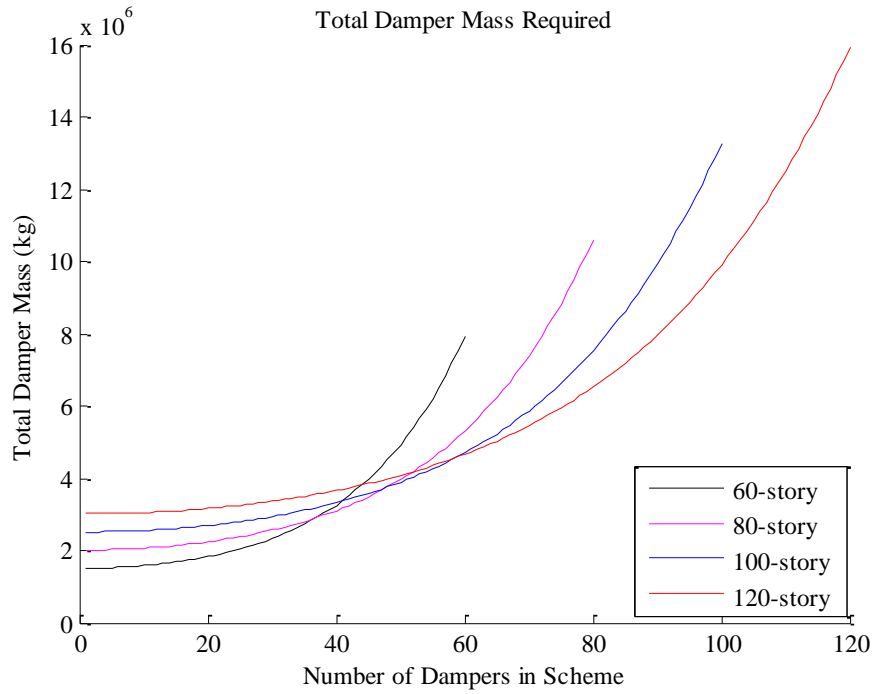


**Figure 4-2: Total Damper Mass Required to Meet 1TMD Performance**

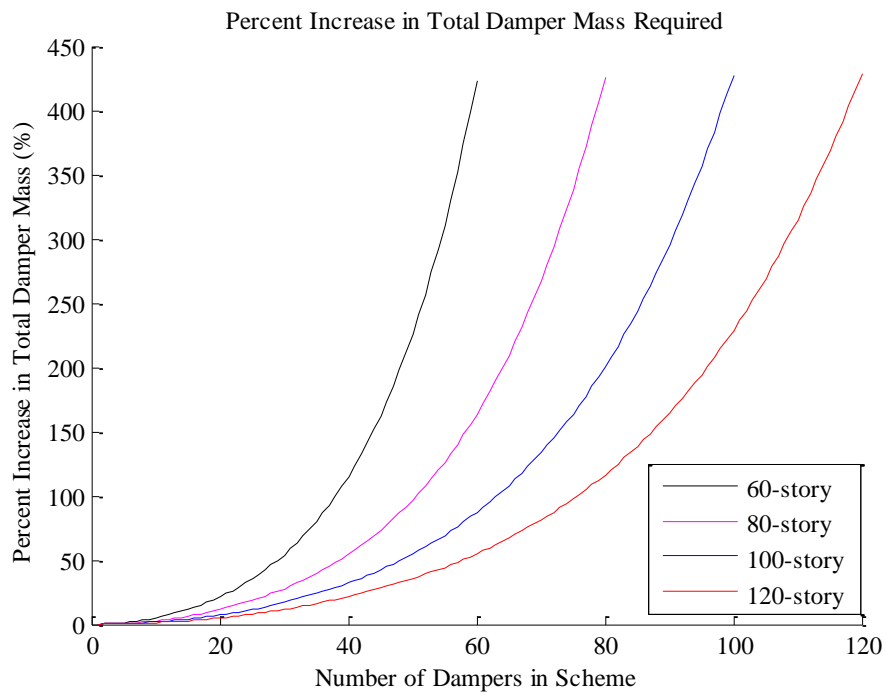


**Figure 4-3: Percent Increase in Total Damper Mass Required to Meet 1TMD Performance**

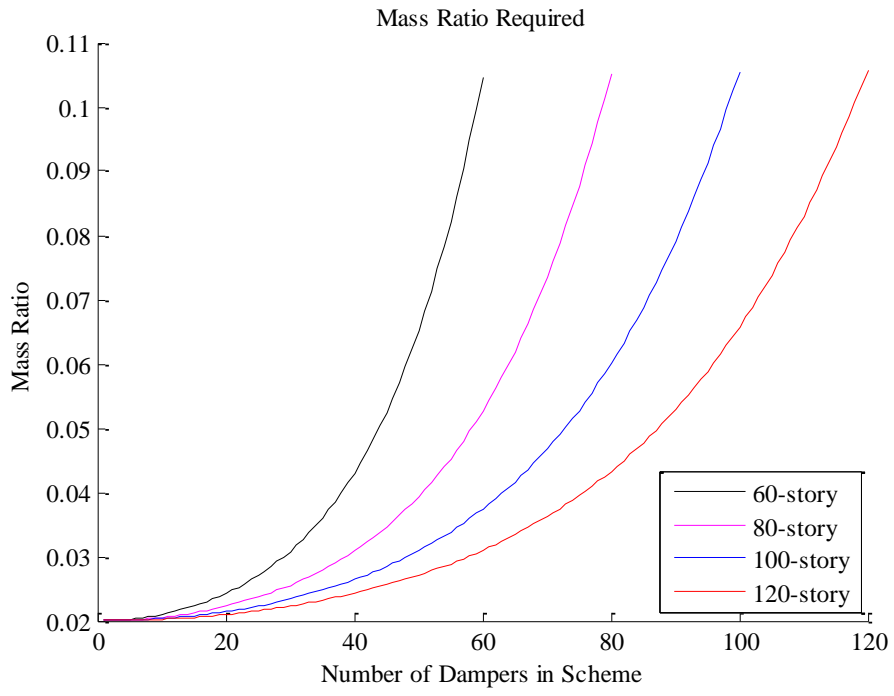


**Figure 4-4: Mass Ratio Required to Meet 1TMD Performance**

## Chapter 5: Damper Footprint

### TMD Footprint

For a comparison of the effect of distribution on the damper footprint, the floor area necessary to accommodate the device is estimated for each scheme and building size. The mass required for equivalent 1TMD performance, along with its damper properties that were calculated in Chapter 4 are used to determine the size of the dampers. A relationship is developed between the damper properties and the dimensions of each mass damping system.

The TMD footprint is calculated based on assumptions of the damper geometry, material properties, and building constraints. While the overall TMD footprint is affected by many ancillary factors, such as space for dashpots, additional structural support, and damper displacement, the floor area considered in this analysis will depend only on the mass of the damper, referred to as the mass footprint. This decision does not affect the optimal damper scheme as long as the other footprint considerations are either negligible relative to the mass footprint or are similarly proportional to the damper mass. Furthermore, the damper displacement decreases as the number of TMDs in the scheme increases and may be reduced further by specifying a damping ratio greater than the optimum parameter. The gross value of the footprint is not considered, since it is the relative space requirement compared among distributions that are studied.

To demonstrate the methodology, the TMDs in this study are assumed to be made of lead and in the shape of a cube. Accordingly, the mass of each damper is converted to a volume ( $V$ ) by dividing it by the density of lead ( $\rho_m = 11,340 \text{ kg/m}^3$ ). Next, the side length ( $s$ ) is calculated by taking the cube root of the volume as long as the length does not exceed the floor height ( $h_f$ ). This condition is in place to ensure the damper can fit within a single story. Then, the footprint is simply the side length squared. If the side length does exceed this threshold value, the height of the damper ( $h_d$ ) is assumed to be equal to the floor height, and the footprint is calculated from the volume divided by this height. This calculation is represented in Eqns. 5-1 through 5-3.

If  $s < h_f$ ,

$$s = \sqrt[3]{\frac{m_d}{\rho_m}} \quad (\text{Eqn. 5-1})$$

$$\text{TMD Footprint} = s^2 \quad (\text{Eqn. 5-2})$$

If  $s > h_f$ ,  $h_d = h_f$ , and then

$$\text{TMD Footprint} = \frac{m_d}{\rho_m h_d} \quad (\text{Eqn. 5-3})$$

This calculation is repeated for each scheme and building height (MATLAB code shown in Appendix C). The footprint per floor of all TMD schemes for the 60-story building is presented in Figure 5-1 (for 80, 100, and 120-story TMD footprint figures, see Appendix D). The footprint data demonstrate a similar conclusion described earlier in the feasibility analysis. At a certain point, the addition of more dampers to the structure has no benefit, and in this case, even increases the damper footprint per floor. The TMD distribution where additional dampers no longer decrease the footprint per floor is the minimum TMD footprint scheme, listed for each building in Table 5-1. Notably, the minimum footprint scheme is the distribution with dampers at about half of the floors. For buildings where dampers are integrated into the building envelope, such as the double skin facade concept, or where the size of the dampers is small enough to be placed in unused space of the building, the minimum footprint scheme may be selected as the optimal distribution for the design.

The footprint per floor is multiplied by the number of TMDs in the scheme to calculate the total footprint, shown in Figure 5-2. As expected, the total footprint increases as the distribution of dampers are placed lower in the building. However, the cost associated with the rentable floor area occupied by the dampers may vary with vertical location and could lead to a cost savings discussed in the following chapter.

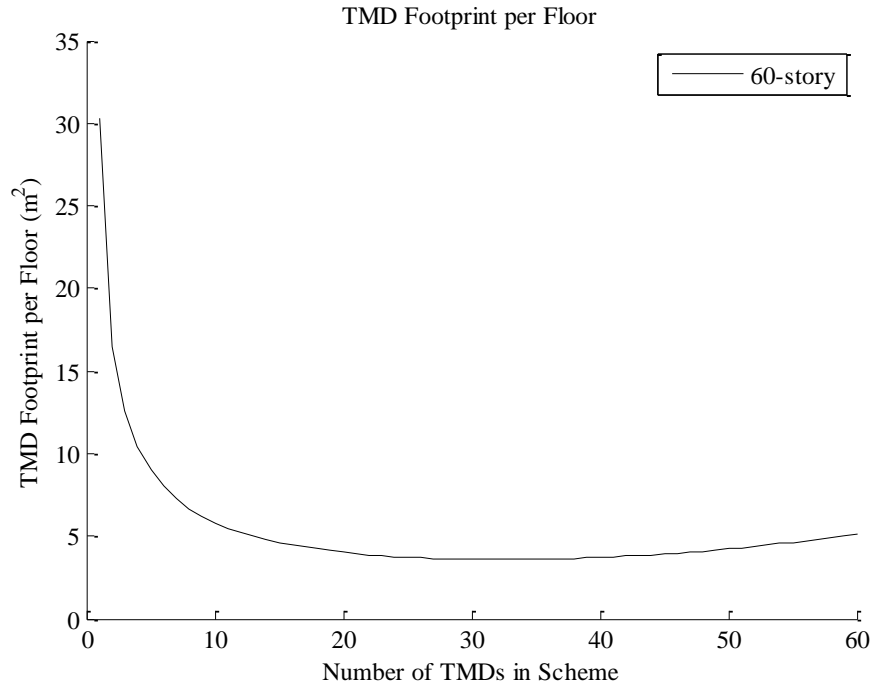


**Figure 5-1: TMD Footprint per Floor for All Schemes in 60-story Building**

**Table 5-1: Minimum TMD Footprint Schemes**

Building Floors	Dampers in Scheme	Mass Footprint per Floor (m <sup>2</sup> )
60	32	3.6
80	43	3.6
100	52	3.6
120	63	3.6

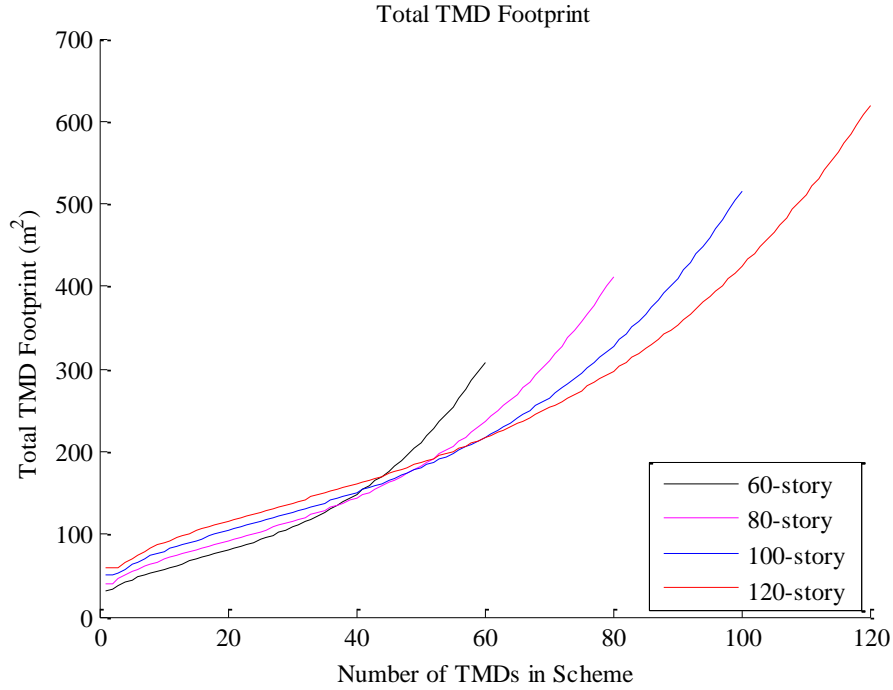


**Figure 5-2: Total TMD Footprint for All Schemes**

### TLCD Footprint

The TLCD footprint is determined from the mass required, the damper natural frequency, and the  $\beta$  factor, assumed to be unity for this study. However, there are several design decisions and assumptions made in calculating all dimensions of the device. First, the total length of the TLCD ( $L_d$ ) is determined from the damper natural frequency ( $\omega_d$ ), which is equal to the length of the horizontal portion ( $B$ ) when  $\beta = 1$ . Then, the damper cross-sectional area ( $A_d$ ) is calculated from the damper mass. After selections are made for the cross-section dimensions, including the depth ( $d$ ) and distance perpendicular to the fluid motion ( $b$ ), the TLCD footprint may be calculated as the product of  $B$  and  $b$ . Eqns. 5-4 through 5-7 show the formulae for this procedure, derived from the manipulation of Eqns. 2-9 and 2-10.

$$L_d = \frac{\alpha g}{\omega_d^2} \quad (\text{Eqn. 5-4})$$

Since  $\beta = 1$ ,  $\alpha = 1$ , and  $L_d = B$ .

$$A_d = \frac{m_d}{\rho' L_d} \quad (\text{Eqn. 5-5})$$

$$b = \frac{A_d}{d} \quad (\text{Eqn. 5-6})$$

$$\text{TLCD Footprint} = B b \quad (\text{Eqn. 5-7})$$

An additional consideration in calculating the TLCD dimensions includes the fluid motion, where the stem height ( $H$ ) must be long enough to contain the fluid when displaced. However, the total height of the damper ( $d + H$ ) must not exceed the floor height. The device is also constrained such that  $B$  and  $b$  must be less than the building width. For the demonstration in this study, schemes where the width constraint is not met are not considered, while the stem height is assumed to be half the floor height and the required TLCD damping constant is assumed to be met through proper adjustment of the orifice opening.

The TLCD footprint per floor for all schemes in the 60-story building is shown in Figure 5-3. The MATLAB calculation for this procedure is shown in Appendix E and the footprint figures for the rest of the buildings are shown in Appendix F. The variation in TLCD footprint per floor is similar to that of the TMD figures in the previous section, but excludes the first few schemes since they do not meet the width constraint. The minimum TLCD footprint scheme for each building is listed in Table 5-2 and is almost identical to the minimum TMD footprint scheme. Similar to the TMD procedure, the total TLCD footprint is calculated and may be used for determining the minimum cost damper distribution, considered in the following chapter. The total TLCD footprint for each building is shown in Figure 5-4.

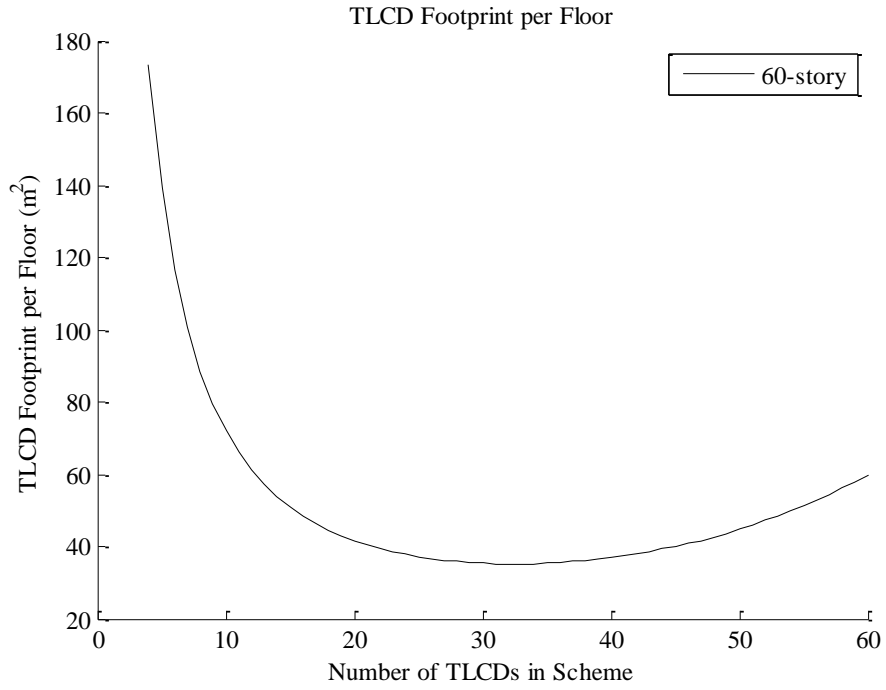


**Figure 5-3: TLCD Footprint per Floor for All Schemes in 60-story Building**

**Table 5-2: Minimum TLCD Footprint Schemes**

Building Floors	Dampers in Scheme	Footprint per Floor (m <sup>2</sup> )
60	32	35
80	43	35
100	54	35
120	65	35

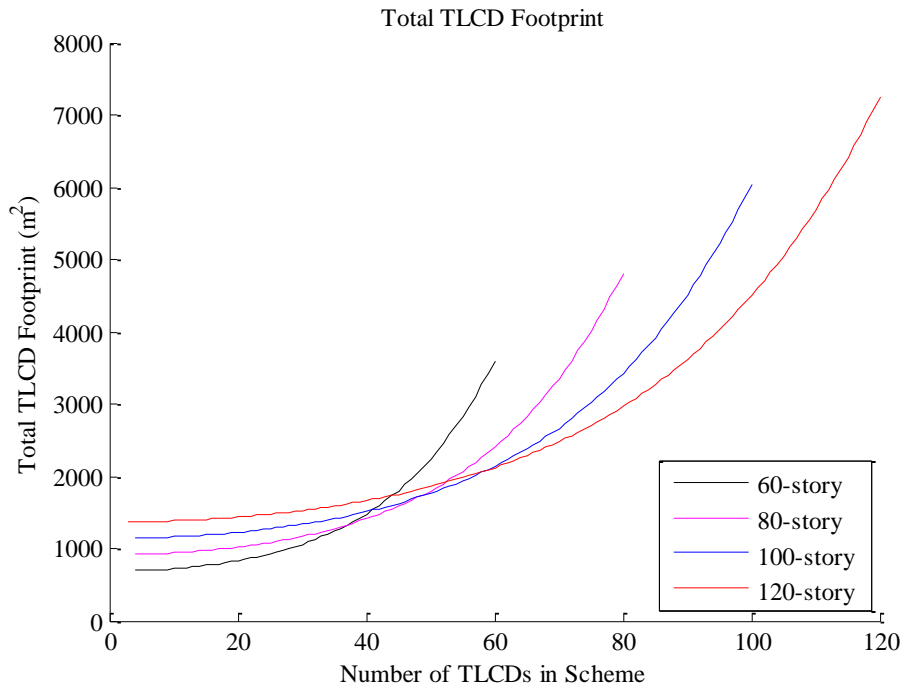


**Figure 5-4: Total TLCD Footprint for All Schemes**



## Chapter 6: Cost Analysis

### Cost Curves

In order to find the cost associated with each distributed damping scheme, it is necessary to know how the cost per area varies along the height of the building. For this analysis, the damper footprint for each floor is multiplied by a cost factor that accounts for the change in price related to the floor level. The value of the cost factor is the price of the floor relative to the bottom floor. In practice, the cost factors are derived from decisions made by the developer or owner and depend on many considerations, such as the building location, the views at each floor, and the prestige of the building. As a demonstration of the methodology, three separate cost curves are assumed and analyzed. Cost curve 1 (C1) represents a building where there is no variation in cost associated with building height. This cost curve is used for comparison as a baseline calculation. Cost curve 2 (C2) has a linear change in cost per square meter, where the top floor is valued at 20 times the cost of the bottom floor. A large cost difference between the top and bottom floor is used to show a more compelling application of distributed damping. Cost curve 3 (C3) is used as a more realistic variation where the cost of the bottom quarter of the building does not vary, the middle of the building varies linearly, and the top quarter of the building increases parabolically. Once again, a substantial cost difference between the bottom, middle, and top sections of the building are assumed. The three cost curves are used for all buildings in this study. The assumed cost curves applied to a 60-story building are shown in Figure 6-1.

From the cost distribution and the damper footprint data, the total cost for each scheme can be calculated. Since only the relative cost, rather than the absolute cost, is necessary to compare the value of each scheme, the cost per square meter is assumed to be unity. The total cost of a scheme is calculated by summing the product of the damper footprint and the corresponding cost factor at each floor. This calculation is expressed in Eqn. 6-1 and repeated for each scheme, building, cost curve, and damping device (MATLAB code in Appendix G).

$$\text{Total Cost} = \sum_{i=n-r}^n (\text{Footprint}_i * CF_i) \quad (\text{Eqn. 6-1})$$

Where  $n$  is the number of floors in the building and  $r$  is the number of dampers.

As an example, the total cost for each scheme in the 60-story building is shown for both TMDs and TLCDs in Figure 6-2 and Figure 6-3, respectively. For cost data on other building heights, see Appendix H.

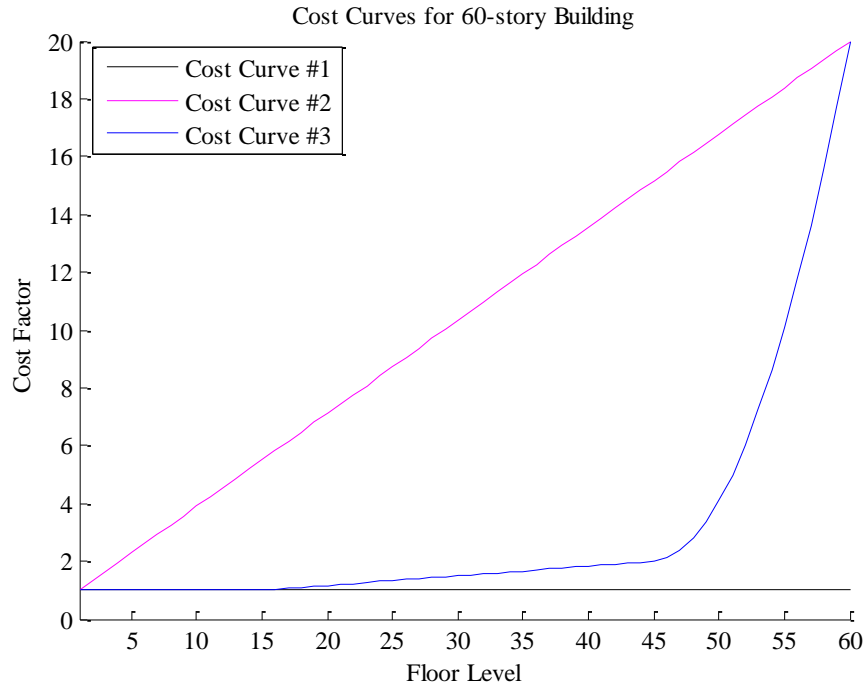


**Figure 6-1: Cost Curves for 60-story Building**

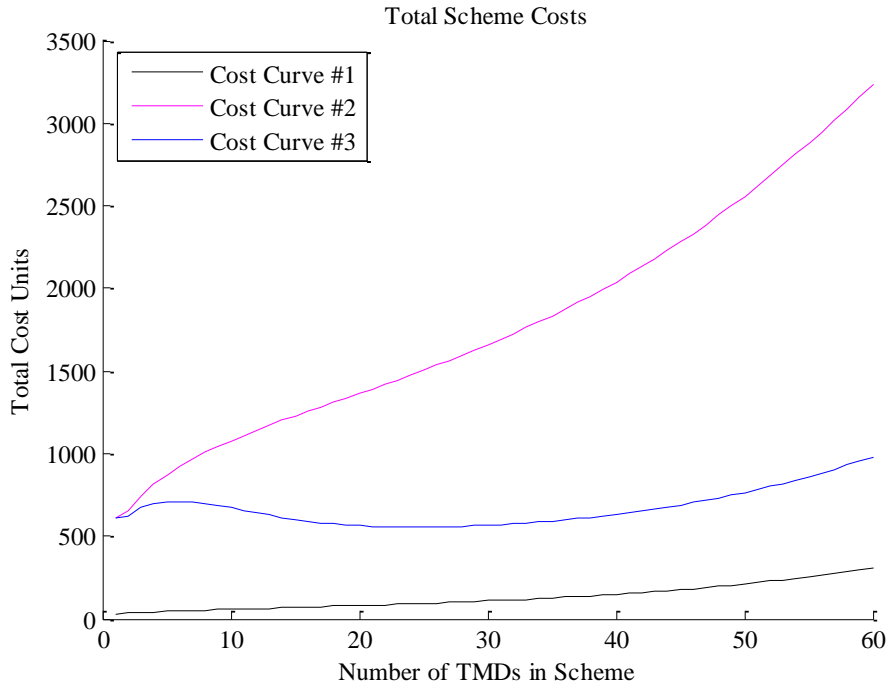


**Figure 6-2: Total Scheme Costs for 60-story Building with Distributed TMDs**

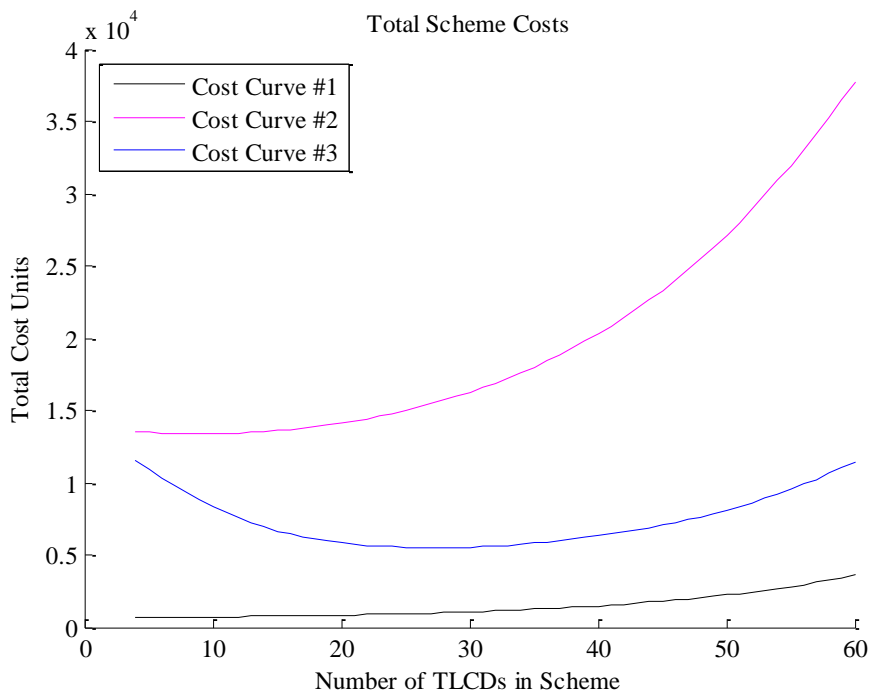


**Figure 6-3: Total Scheme Costs for 60-story Building with Distributed TLCDs**

## Optimal Scheme

In this study, the optimal scheme is considered to be the damper distribution where the total cost of the scheme is minimal. As shown in the previous section, this optimal scheme is dependent on the footprint requirement of the damping devices and the cost distribution of the building. In Table 6-1, the minimum cost scheme is presented for each cost curve, building, and device. As expected, for all buildings, the optimal TMD scheme associated with the first cost curve is the contemporary 1TMD design scheme and for TLCDs, it is the first scheme that meets the building constraints. Since there is no cost benefit to moving the dampers lower in the building, the scheme with the minimum total footprint is the optimal design. The minimum cost scheme using the second cost curve involves more dampers as the building height increases. The optimal scheme in this demonstration varies more from the conventional design with TLCDs rather than TMDs. Finally, the third cost curve, which represents a significant variation in top floor value, results in a large distribution of both damping systems.

**Table 6-1: Optimal Schemes for All Buildings, Cost Curves, and Damping Systems**

	Building Floors	Dampers in Scheme		
		C1	C2	C3
TMDs	60	1	1	24
	80	1	2	33
	100	1	2	41
	120	1	3	48
TLCDs	60	4	9	27
	80	4	12	36
	100	4	15	45
	120	3	18	54

The damper footprint and dimensions of the optimal schemes are listed in Table 6-2. The 120-story building is used as a representative example. As shown in this demonstration, not only can distributed damping be the least cost option from its use of less expensive floor area, but it can lead to a much smaller and more convenient device to manufacture and implement.

**Table 6-2: Damper Dimensions of Optimal Scheme for 120 story Building**

	TMD			TLCD		
	Dampers	Footprint (m <sup>2</sup> )	s (m)	Dampers	Footprint (m <sup>2</sup> )	A <sub>d</sub> (m <sup>2</sup> )
C1	1	60	7.8	3	460	500
C2	3	20	4.5	18	79	29
C3	48	3.8	1.9	54	36	13



## Chapter 7: Conclusions

### Discussion of Results

In the design of a distributed mass damping system, the damper properties and vertical placement are design parameters that may be optimized to effectively control displacements and accelerations from dynamic excitations in tall buildings. However, there are additional considerations in finding the optimal distribution, including the size of the damper and value of the space occupied by the device. This study presents a methodology where these considerations may be implemented into the design process by calculating the footprint and cost of each scheme of TMDs and TLCDs and finding the minimum cost solution. In order to execute this design procedure, a derivation of the displacement and acceleration profile of a structure with distributed damping was developed, along with a program that could simulate the structural response of any given damping distribution and loading.

The methodology was demonstrated on 60, 80, 100, and 120-story buildings, loaded with a periodic wind load to represent vortex shedding excitations. Damper schemes ranging from the contemporary 1TMD design approach to a scheme with dampers at every floor were developed and, under resonant conditions, were analyzed for their performance. With maximum acceleration as the design constraint, the damper mass of each scheme was iterated until equivalent performance was achieved compared to the 1TMD scheme. TMD and TLCD footprints were calculated from the design parameters and summed to find the total footprint of each scheme. Then, a cost analysis was performed by assuming several cost distributions of the buildings. By summing the product of the each damper footprint with a cost factor that quantifies the relative cost of the floor, the total cost of each scheme was calculated and compared to find the optimal distribution. It was found that for buildings with significant variation in cost in the upper floors, distributed damping is not only the least cost solution, but also leads to conveniently small devices.

The procedure developed in this study may be used by developers and engineers early in the design process to determine the best strategy for motion control of the building. For example, the mass necessary for a given damper distribution may be used as an additional consideration to select a mass ratio for the design. This gives greater flexibility to the design team in determining what type of damping system to use and how it will be implemented into the design concept of

the building. Also, for integrative design concepts where motion control is incorporated into the façade or structural components, the methodology may be altered to select the minimum footprint scheme as the optimal distribution. When distribution schemes are designed to employ very small devices, almost no usable floor area is occupied by the dampers and could even be placed in hidden locations, such as mechanical rooms or ceilings. Distributed schemes also increase motion control reliability. By dividing up the damper mass, a failure or malfunction of one device does not compromise the entire damping strategy for the building.

Implementing distributed damping schemes have several benefits when compared to a 1TMD scheme. Not only are the motion control devices smaller and easier to handle, but they are placed lower in the building. This makes installing the dampers less of a disruptive activity and is safer than lifting a much larger mass into an upper floor. Distributed damping could also be utilized as the building is erected. When dynamic construction loads are a design consideration, dampers may be adaptively tuned to the building's changing fundamental frequency. Rather than a large mass that requires extensive structural support, the use of smaller dampers reduces the additional stiffness necessary to resist their dead loads. Furthermore, the use of modular devices is advantageous in manufacturing the dampers and is more convenient when organizing the installation of the devices.

## **Future Research**

The distributed damping methodology presented in this study may be further developed by generalizing the governing equations and derivation to include additional dynamic loading scenarios, such as earthquakes, random excitations, or other non-periodic loads. While the preceding demonstration considered damping schemes where consecutive floors, starting at the top, were installed with motion control devices, to be complete in finding the optimal scheme, it is necessary to evaluate all possible combinations. These distributions could include schemes where there are devices at every other or every few floors, and schemes where there are not necessarily dampers on the top floors.

Distributed damping performance in this study could be improved through numerical optimization of the frequency and damping ratio, rather than using optimal values of an equivalent SDOF structure. These optimal parameters could be found by developing transfer functions relating the loading to the acceleration or displacement response and finding the values

for which the dynamic amplification factor is minimal. This procedure is necessary for each structure and damping scheme, and would result in a smaller required mass, thereby increasing the cost benefits of distributed damping.

For a more robust motion control strategy, a similar technique used for MTMD systems may be applied to distributed damping. By varying the natural frequency of the devices, the dampers may be effective for a wider range of excitation frequencies and would be less sensitive to the frequency ratio. Additionally, distributing the damper mass horizontally can further decrease the size and increase effectiveness of the dampers. The methodology in this study may then be expanded to find the optimal scheme of horizontal and vertical distributions with consideration of the damper footprint, cost, and range of excitation frequencies.

Demonstrations of the distributed damping methodology should be applied to buildings with variable mass and stiffness, such as structures with tapers and setbacks, or a parabolic stiffness distribution. While the buildings used in this study had constant mass and stiffness, it is more realistic to analyze structures with irregular properties. Furthermore, rather than neglecting inherent damping in the building, analysis should be performed on the effect of structural damping on the optimal scheme and perform a cost analysis that compares a combination of different motion control strategies. An assumed mass ratio of 2% was used for this demonstration but a variation in this parameter may lead to a new optimal scheme and should also be studied for its effect.

Damper footprint calculations for TMDs in this study only considered the volume of lead necessary to provide the mass required, while TLCD footprints were determined from damper properties only using the width as a constraint. For TLCDs, this constraint could be met by decreasing the  $\beta$  parameter and therefore increasing the stem height and decreasing performance. However, for actual implementation of each device, the damper or fluid displacement could be a significant constraint. A further iteration of design would require a check of this displacement and could be satisfied by increasing the damping ratio above the optimum value and consequently accepting a possible loss in effectiveness. It was also assumed that the TLCD damping parameter could be met by specifying an orifice opening ratio that provides equivalent viscous damping. Hydrodynamic analysis is necessary to confirm that a realistic orifice opening ratio exists that could meet the specified performance.

Supplemental factors that contribute to the footprint of the devices were not considered in this study but may affect the results if they are not similarly proportional to an increase in damper mass. Therefore, further study should be performed on the space required for dashpots, effective springs, additional structural support, and safety clearance. Also, a review of TMD and TLCD devices currently in production from manufacturers would be beneficial in determining the actual footprint and how damper size varies with mass.

When performing a cost analysis, a more accurate comparison of distributed schemes would require empirical cost data from several buildings currently in use. It could then be studied how the value of real estate varies with floor height and the effect of building location, prestige, total building height, and other characteristics on the vertical cost distribution. Predictions could then be made on what types of buildings are best suited for a distributed damper scheme. A cost analysis should also include savings and expenditures from construction. Associating a cost with the construction effort necessary to implement the devices and how it changes with mass and vertical location would provide a more precise cost of each damper scheme for comparison.

With the preceding improvements to the methodology, a thorough design of distributed mass damping systems may be performed to find the optimal scheme for motion control of tall buildings.

## Appendix A: Simulator

```
%Simulator with arbitrary number of dampers and nodes.
%Constant m, md, c, cd, k, and kd.
%Equal total mass considered for each damper scheme.

%Load stiffness that meets design constraint. (Umax=H/400)
load('kreq.mat')

NN=[60 80 100 120];%Number of nodes/stories used for this analysis.

%Calculate for all buildings.
for index=1:size(NN,2)
    N=NN(index);

    mm=2500000;%(kg) Assumed mass per floor

    %Assemble local matrices from structural properties.
    m=0;%reset for iteration
    m(1:N)=mm;
    m=diag(m);
    kdiag(1:N)=2;
    kupper(1:N-1)=-1;
    klower(1:N-1)=-1;
    k=0;%reset for iteration
    k=diag(kdiag)+diag(kupper,1)+diag(klower,-1);
    k(N,N)=1;
    kk=kreq(index);%(N/m)
    k=kk*k;

    %Eigenvalues
    [phi,ohm2]=eig(k,m);
    phi=phi(:,1)/phi(N,1);%Normalize mode shape such that max value is one.
    modalmass=phi(:,1)'*m*phi(:,1);
    modalstiffness=phi(:,1)'*k*phi(:,1);
    w=sqrt(ohm2(1,1));%(rad/s)

    %Inherent Damping. Assume proportional to stiffness.
    ksi=0;%Assume no inherent damping.
    modal damping=2*ksi*w*modalmass;
    alpha=2*ksi/w;
    c=alpha*k;

    %Specify loading. Assume uniform load.
    wp=1500;%(Pa) Typical wind pressure
    floor=4.4;%Assume 4.4m floor height
    totalheight=floor*N;
    B=totalheight/7;%Building width. Assume slenderness ratio of 1:7
    distload=wp*B;%(N/m)
    pp=wp*B*floor;%(N) Resolve distributed load into point loads.

    %Consider schemes that have only one damper through those with dampers
    %at each floor.
```

```

for TMD=1:N%TMD=number of equal mass TMDs at each floor starting at top
%TMD design
massratio=0.02;%Assumed to be 2%
mmd_total=massratio*modalmass;%Mass necessary if only 1TMD at top
mmd{index}(TMD)=mmd_total/TMD;%Equal TMD mass at each floor
if ksi==0
    fopt=sqrt(1-0.5*massratio)/(1+massratio);
    ksidopt=sqrt(massratio*(3-
sqrt(0.5*massratio))/(8*(1+massratio)*(1-0.5*massratio)));
else
    %Curve fitting from Tsai & Lin (1993)
    fopt=(sqrt(1-0.5*massratio)/(1+massratio)+sqrt(1-2*ksi^2)-1)-
(2.375-1.034*sqrt(massratio)-0.426*massratio)*ksi*sqrt(massratio)-(3.730-
16.903*sqrt(massratio)+20.496*massratio)*ksi^2*sqrt(massratio);
    ksidopt=sqrt(3*massratio/(8*(1+massratio)*(1-
0.5*massratio)))+(0.151*ksi-0.170*ksi^2)+(0.163*ksi+4.980*ksi^2)*massratio;
end
%Damper properties
wd=fopt*w;
kkd{index}(TMD)=wd^2*mmd{index}(TMD);
ccd{index}(TMD)=2*ksidopt*wd*mmd{index}(TMD);

%Create local matrices from damper properties.
md=0;%reset for iteration
md(1:TMD)=mmd{index}(TMD);
md=diag(md);
cd=0;%reset for iteration
cd(1:TMD)=ccd{index}(TMD);
cd=diag(cd);
kd=0;%reset for iteration
kd(1:TMD)=kkd{index}(TMD);
kd=diag(kd);

%Create load vector.
W=0;%reset for iteration
W(1:N+TMD)=w;%Assume loaded at structure's first natural frequency.
W2=0;%reset for iteration
W2(1:N+TMD)=w^2;
W=diag(W);
W2=diag(W2);
p=0;%reset for iteration
p(1:N,1)=pp;
p(N,1)=pp/2;

%Create Connectivity matrix and adjust local matrices accordingly.
E=zeros(N,TMD);
nTMD=0;%reset for iteration
nTMD(1:TMD)=1;
nTMD=diag(nTMD);
E(N+1-TMD:N,1:TMD)=nTMD;
md_prime=E*md*E';
md_dprime=E*md;

%Create global matrices.
z=zeros(N,TMD);
z1=zeros(N);

```

```

z2=zeros(TMD);
zz=zeros(TMD,1);
M=[m+md_prime z; z' md];
Ms=[z1 md_dprime; md_dprime' z2];
K=[k z; z' kd];
C=[c z; z' cd];
P=[p;zz];

%Apply derivation for distributed damping response.
U=abs((K-(M+Ms)*W2+1i*C*W)^-1*P);%(m)
A=W2*U*(1/9.81);%(as a percent of g)

Umax(TMD)=max(U(1:N));%Find max displacement for each scheme.
Amax(TMD)=max(A(1:N));%Find max acceleration for each scheme.
end
Umaxnorm=(Umax/Umax(1)-1)*100;%Normalized max displacement to 1TMD case.
Amaxnorm=(Amax/Amax(1)-1)*100;%Normalized max acceleration to 1TMD case.
end

```



## Appendix B: Damper Mass Iteration

```
%Design 1TMD system, calculate response, then use that max acceleration
%as a performance constraint. Iterate damper mass for each scheme to meet
%1TMD performance.

%Load stiffness that meets design constraint. (Umax=H/400)
load('kreq.mat')

NN=[60 80 100 120];%Number of nodes/stories used for this analysis.

%Calculate for all buildings.
for index=1:size(NN,2)
    N=NN(index);

    mm=2500000;%(kg) Assumed mass per floor

    %Assemble local matrices from structural properties.
    m=0; %reset for iteration
    m(1:N)=mm;
    m=diag(m);
    k=0; %reset for iteration
    kdiag(1:N)=2;
    kupper(1:N-1)=-1;
    klower(1:N-1)=-1;
    k=diag(kdiag)+diag(kupper,1)+diag(klower,-1);
    k(N,N)=1;
    kk=kreq(index);%(N/m)
    k=kk*k;

    %Eigenvalues
    [phi,ohm2]=eig(k,m);
    phi=phi(:,1)/phi(N,1);%Normalize mode shape such that max value is one.
    modalmass=phi(:,1)'*m*phi(:,1);
    modalstiffness=phi(:,1)'*k*phi(:,1);
    w=sqrt(ohm2(1,1));

    %Inherent Damping. Assume proportional to stiffness.
    ksi=0;%Assume no inherent damping.
    modal damping=2*ksi*w*modalmass;
    alpha=2*ksi/w;
    c=alpha*k;

    %Specify loading. Assume uniform load.
    wp=1500;%(Pa) Typical wind pressure
    floor=4.4;%Assume 4.4m floor height.
    totalheight=floor*N;
    B=totalheight/7;%Building width. Assume slenderness ratio of 1:7.
    distload=wp*B;%(N/m)
    pp=wp*B*floor;%(N) Resolve distributed load into point loads.

    %TMD Design
    massratio=0.02;%Assumed to be 2%
```

```

mmdl=massratio*modalmass;%Mass necessary if only 1TMD
if ksi==0
    fopt1=sqrt(1-0.5*massratio)/(1+massratio);
    ksidopt1=sqrt(massratio*(3-sqrt(0.5*massratio)))/(8*(1+massratio)*(1-
0.5*massratio));
else
    %Curve fitting from Tsai & Lin (1993)
    fopt1=(sqrt(1-0.5*massratio)/(1+massratio)+sqrt(1-2*ksi^2)-1)-(2.375-
1.034*sqrt(massratio)-0.426*massratio)*ksi*sqrt(massratio)-(3.730-
16.903*sqrt(massratio)+20.496*massratio)*ksi^2*sqrt(massratio);
    ksidopt1=sqrt(3*massratio/(8*(1+massratio)*(1-
0.5*massratio)))+(0.151*ksi-0.170*ksi^2)+(0.163*ksi+4.980*ksi^2)*massratio;
end
%Damper properties
wd1=fopt1*w;
kkd1=wd1^2*mmdl;
ccd1=2*ksidopt1*wd1*mmdl;

%Create local matrices from damper properties.
md=0; %reset for iteration
md=mmdl;
md=diag(md);
cd=0; %reset for iteration
cd=ccd1;
cd=diag(cd);
kd=0; %reset for iteration
kd=kkd1;
kd=diag(kd);

%Create load vector.
W=0; %reset for iteration
W(1:N+1)=w;%Assume loaded at structure's first natural frequency.
W2=0; %reset for iteration
W2(1:N+1)=w^2;
W=diag(W);
W2=diag(W2);
p=0; %reset for iteration
p(1:N,1)=pp;
p(N,1)=pp/2;

%Create Connectivity matrix and adjust local matrices accordingly.
E=zeros(N,1);
nTMD=1;
nTMD=diag(nTMD);
E(N,1)=nTMD;
md_prime=E*md*E';
md_dprime=E*md;

%Create global matrices.
M=0; Ms=0;K=0;C=0; P=0; %reset for iteration
zz=zeros(N,1);
zz1=zeros(N);
zz2=zeros(1);
zzz=zeros(1,1);
M=[m+md_prime zz; zz' md];
Ms=[zz1 md_dprime; md_dprime' zz2];

```

```

K=[k zz; zz' kd];
C=[c zz; zz' cd];
P=[p; zzz];

%Apply derivation for distributed damping response.
U=abs((K-(M+Ms)*W2+1i*C*W)^-1*P);%(m)
A=W2*U*(1/9.81);%(as a percent of g)

U_star=max(U(1:N));
A_star=max(A(1:N));%Acceleration is used as design constraint.

for TMD=1:N
    W=0;
    W(1:N+TMD)=w;
    W2=0;
    W2(1:N+TMD)=w^2;
    W=diag(W);
    W2=diag(W2);
    %Iterate through damper mass.
    for mmd=100:100:10000000%(kg)
        %TMD Design
        mmd_total=mmd*TMD;
        massratio=mmd_total/modalmass;
        if ksi==0
            fopt=sqrt(1-0.5*massratio)/(1+massratio);
            ksidopt=sqrt(massratio*(3-
sqrt(0.5*massratio))/(8*(1+massratio)*(1-0.5*massratio)));
        else
            fopt=(sqrt(1-0.5*massratio)/(1+massratio)+sqrt(1-2*ksi^2)-1)-
(2.375-1.034*sqrt(massratio)-0.426*massratio)*ksi*sqrt(massratio)-(3.730-
16.903*sqrt(massratio)+20.496*massratio)*ksi^2*sqrt(massratio);
            ksidopt=sqrt(3*massratio/(8*(1+massratio)*(1-
0.5*massratio)))+(0.151*ksi-0.170*ksi^2)+(0.163*ksi+4.980*ksi^2)*massratio;
        end
        wd=fopt*w;
        kkd=wd^2*mmd;
        ccd=2*ksidopt*wd*mmd;

        %Create local matrices.
        md=0;
        md(1:TMD)=mmd;
        md=diag(md);
        cd=0;
        cd(1:TMD)=ccd;
        cd=diag(cd);
        kd=0;
        kd(1:TMD)=kkd;
        kd=diag(kd);

        %Create connectivity matrix.
        E=zeros(N,TMD);
        nTMD=0;
        nTMD(1:TMD)=1;
        nTMD=diag(nTMD);
        E(N+1-TMD:N,1:TMD)=nTMD;
    end
end

```

```

md_prime=E*md*E';
md_dprime=E*md;

%Create global matrices.
z=zeros(N,TMD);
z1=zeros(N);
z2=zeros(TMD);
zz=zeros(TMD,1);
M=[m+md_prime z; z' md];
Ms=[z1 md_dprime; md_dprime' z2];
K=[k z; z' kd];
C=[c z; z' cd];
P=[p;zz];

U=abs((K-(M+Ms)*W2+1i*C*W)^-1*P);
A=W2*U*(1/9.81);

Umax=max(U(1:N));%Find max displacement for each scheme.
Amax=max(A(1:N));%Find max acceleration for each scheme.

%If the maximum acceleration meets the 1TMD performance,
%collect the damper properties as results.
if Amax<=A_star
    mmd_req(TMD)=mmd;%Damper mass
    Uresults{index}{TMD}=U;%Displacement profile
    Aresults{index}{TMD}=A;%Acceleration profile
    kkd_req{index}(TMD)=kkd;%Damper stiffness
    ccd_req{index}(TMD)=ccd;%Damping constant
    wd_req{index}(TMD)=wd;%Damper frequency
    break
end
end
%Total mass required
mmd_total_req{index}(TMD)=mmd_req(TMD)*TMD;
%Mass ratio required
massratio_req{index}(TMD)=mmd_total_req{index}(TMD)/modalmass;
end
%Percent increase in mass required compared to 1TMD scheme
mmd_total_inc{index}=(mmd_total_req{index}/mmd_total_req{index}(1)-
1)*100;
end

```

## Appendix C: TMD Footprint Calculation

```
%Calculate TMD footprint.

%Load previous results.
load('mmd_req.mat')%Damper mass required for equivalent 1TMD performance

%Define constants necessary for calculation.
density=11340;%(kg/m3) Density of TMD material. Assume lead mass.
floor=4.4;%(m) Floor height

NN=[60 80 100 120];%Number of nodes/stories used for this analysis.

%Calculate for all buildings.
for index=1:size(NN,2)
    N=NN(index);
    %Calculate for all schemes.
    for TMD=1:N
        %Find side length
        s=(mmd_req{index}(TMD)/density)^(1/3);%Initially assume cube shape.
        %If TMD is taller than the floor height, then set TMD height equal
        %to floor height and calculate the other two dimensions.
        if s>floor
            h{index}(TMD)=floor;
            side{index}(TMD)=sqrt(mmd_req{index}(TMD)/(floor*density));
        else
            h{index}(TMD)=s;
            side{index}(TMD)=s;
        end
        footprint{index}(TMD)=side{index}(TMD)*side{index}(TMD);
    end
    %Find scheme where adding more TMDs no longer decreases footprint.
    %This is the minimum footprint scheme.
    minFootprint(index)=min(footprint{index});
    [one minFootprintScheme(index)]=min(footprint{index});
end
```



## Appendix D: TMD Footprint per Floor

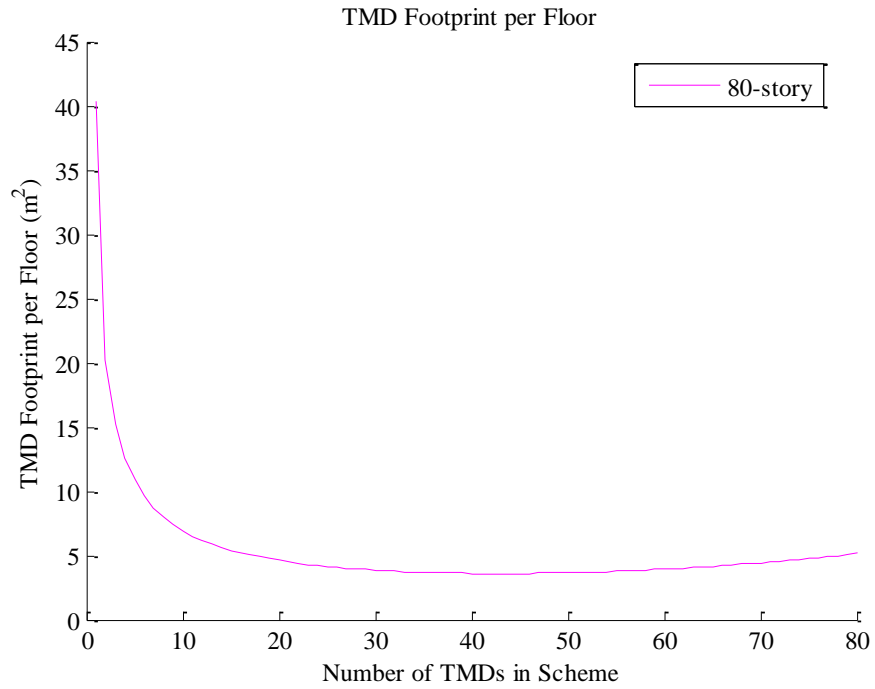


**Figure D-1: TMD Footprint per Floor for All Schemes in 80-story Building**

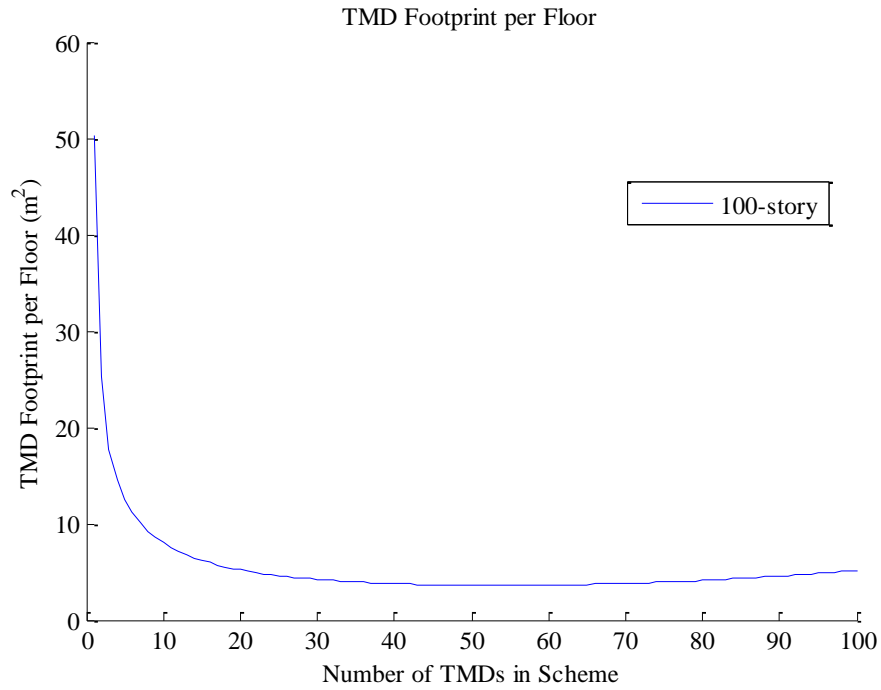


**Figure D-2: TMD Footprint per Floor for All Schemes in 100-story Building**

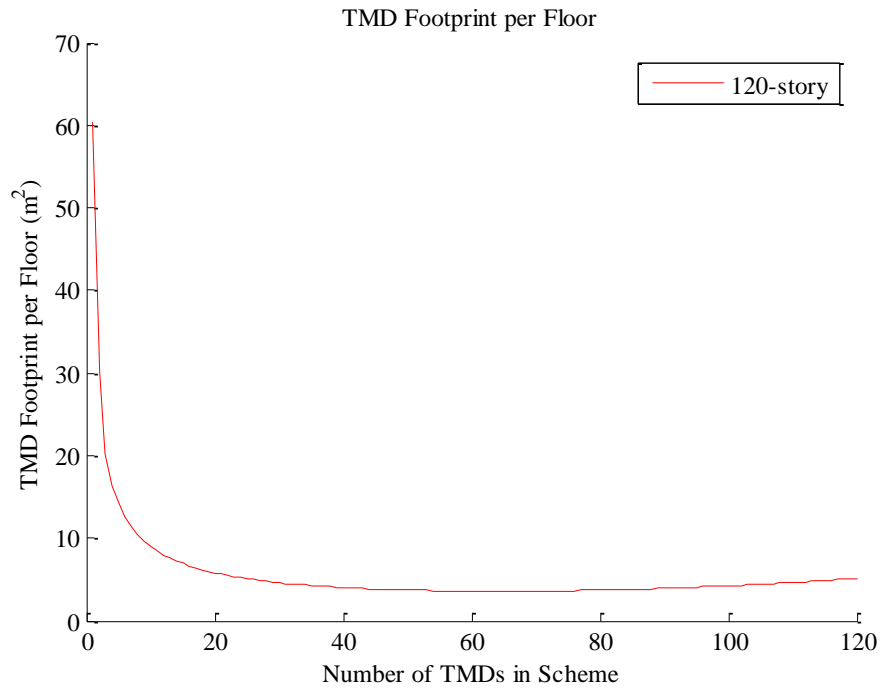


**Figure D-3: TMD Footprint per Floor for All Schemes in 120-story Building**

## Appendix E: TLCD Footprint Calculation

```
%Calculate TLCD footprint.

%Load previous results.
load('mmd_req.mat')%Damper mass required for equivalent 1TMD performance
load('wd_req.mat')%Damper frequency
load('ccd_req.mat')%Damping constant

%Define constants necessary for calculation.
g=9.81;%(m/s2)
rho=1000;%(kg/m3) Mass density of water
beta=1;%Assume beta=1 for best performance and comparable derivation to TMD
floorheight=4.4;%(m)

NN=[60 80 100 120];%Number of nodes/stories used for this analysis.

%Assume height of horizontal section is half of the floor height.
h=floorheight/2;

%Determine geometric constant.
if beta==1
    a=1;
else
    a=2;
end

%Calculate for all buildings.
for index=1:size(NN,2)
    N=NN(index);
    %Introduce constraints from building dimensions.
    totalheight=floorheight*N;
    B=totalheight/7;
    %Calculate for all schemes.
    for TLCD=1:N
        Ld{index}(TLCD)=a*g/wd_req{index}(TLCD).^2;%(m) Total TLCD length
        BBd=beta*Ld{index}(TLCD);%(m) Length of horizontal section
        %Check whether it fits within the building width.
        if BBd<=B
            Bd{index}(TLCD)=BBd;
        else
            %If it does not fit, it is not considered in the analysis.
            Bd{index}(TLCD)=1/0;
        end
        %Calculate cross-sectional area (m2)
        Ad{index}(TLCD)=mmd_req{index}(TLCD)/(rho*Ld{index}(TLCD));
        bbd=Ad{index}(TLCD)/h;%(m) Width perpendicular to fluid motion
        %Check whether it fits within the building width.
        if bbd<=B
            bd{index}(TLCD)=bbd;
        else
            %If it does not fit, it is not considered in the analysis.
            bd{index}(TLCD)=1/0;
        end
        footprint_TLCD{index}(TLCD)=bd{index}(TLCD)*Bd{index}(TLCD);
    end
end
```

```
end
%Find scheme where adding more TLCDs no longer decreases footprint.
%This is the minimum footprint scheme.
minFootprint_TLCD(index)=min(footprint_TLCD{index});
[one minFootprintScheme_TLCD(index)]=min(footprint_TLCD{index});
end
```

## Appendix F: TLCD Footprint per Floor

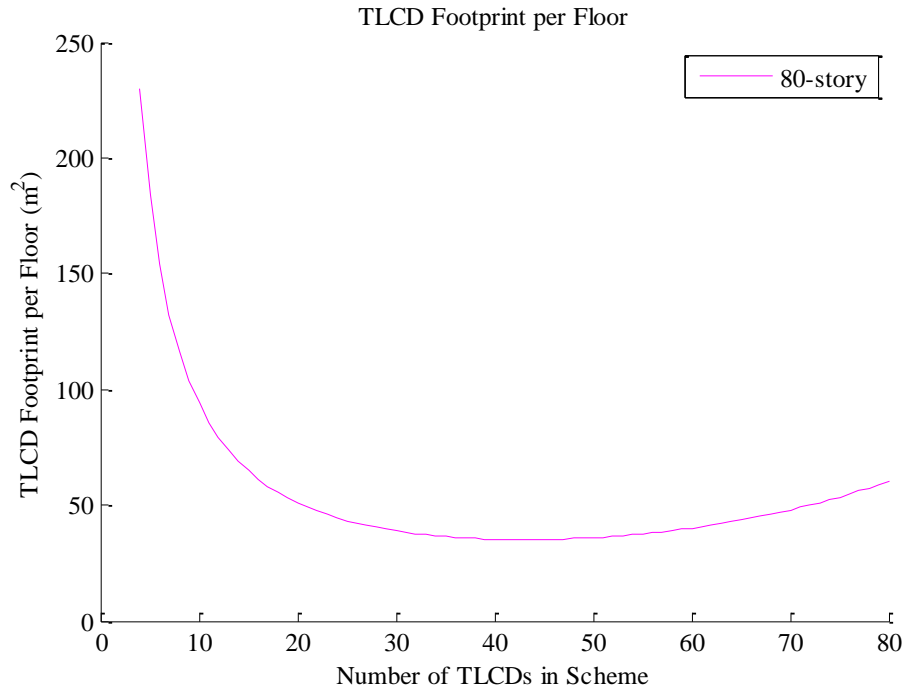


Figure F-1: TLCD Footprint per Floor for All Schemes in 80-story Building

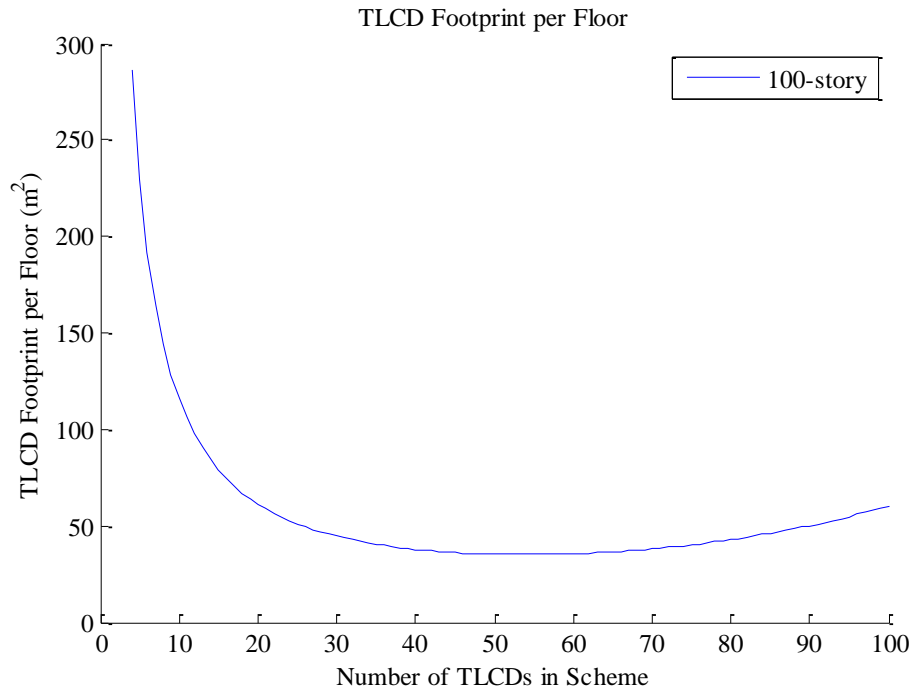
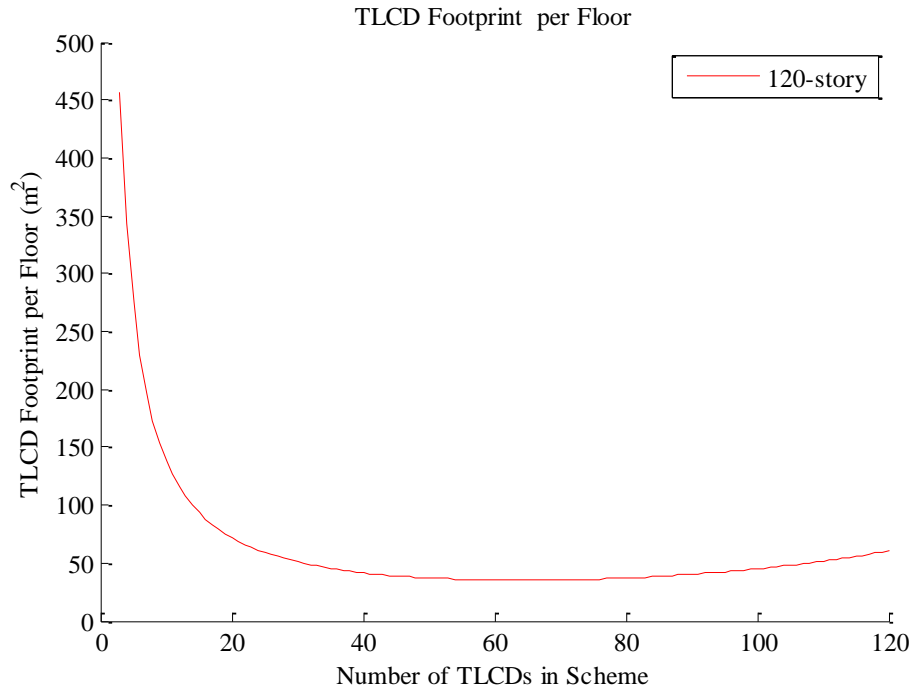


Figure F-2: TLCD Footprint per Floor for All Schemes in 100-story Building



**Figure F-3: TLCD Footprint per Floor for All Schemes in 120-story Building**

## Appendix G: Cost Calculation

```

%Calculate the total cost of each scheme based on the value of the floor
%area occupied by the device.

%Load previous results.
load('footprint.mat')%(m2) TMD footprint for each scheme
load('footprint_TLCD.mat')%(m2) TLCD footprint for each scheme

%Input cost variation values.
Q2=20;%Top floor is Q2 times as expensive as bottom floor.
Q1=2;%Top of the middle section is Q1 times as expensive as bottom floor.

NN=[60 80 100 120];%Number of nodes/stories used for this analysis.

%Calculate for all buildings.
for index=1:size(NN,2)
    N=NN(index);
    %Calculate for all schemes.
    for TMD=1:N
        %Calculate total footprint
        totalfootprint_TMD{index}(TMD)=footprint{index}(TMD)*TMD;
        totalfootprint_TLCD{index}(TMD)=footprint_TLCD{index}(TMD)*TMD;
        %Calculate cost curve 1. (Constant)
        CF_c{index}(1:N)=1;
        %Calculate cost curve 2. (Linear)
        floor_c=1:N;
        CF_l{index}(1:N)=(Q2-1)/(N-1).*(floor_c-1)+1;
        %Calculate cost curve 3. (Constant, linear, then parabolic)
        floor_p1=.25*N+1:.75*N;
        floor_p2=.75*N+1:N;
        CF_p{index}(1:.25*N)=1;
        CF_p{index}(.25*N+1:.75*N)=(Q1-1)/(.5*N).*(floor_p1-.25*N)+1;
        alef=(Q2-Q1-.5*(Q1-1))/(.25*N)^2;
        bet=(Q1-1)/(.5*N);
        CF_p{index}(.75*N+1:N)=alef.*(floor_p2-.75*N).^2+bet*(floor_p2-
        .75*N)+Q1;
        %Calculate total cost for all three cost curves and both systems.
        cost_TMD_c{index}(TMD)=footprint{index+4}(TMD)*sum(CF_c{index}(N+1-
        TMD:N));
        cost_TMD_l{index}(TMD)=footprint{index+4}(TMD)*sum(CF_l{index}(N+1-
        TMD:N));
        cost_TMD_p{index}(TMD)=footprint{index+4}(TMD)*sum(CF_p{index}(N+1-
        TMD:N));

        cost_TLCD_c{index}(TMD)=footprint_TLCD{index+4}(TMD)*sum(CF_c{index}(N+1-
        TMD:N));

        cost_TLCD_l{index}(TMD)=footprint_TLCD{index+4}(TMD)*sum(CF_l{index}(N+1-
        TMD:N));

        cost_TLCD_p{index}(TMD)=footprint_TLCD{index+4}(TMD)*sum(CF_p{index}(N+1-
        TMD:N));
        %Find minimum cost scheme for TMD footprint schemes.
        [one mincostScheme_TMD_c(index)]=min(cost_TMD_c{index});
    end
end

```

```
mincost_TMD_c(index)=min(cost_TMD_c{index});
[one mincostScheme_TMD_l(index)]=min(cost_TMD_l{index});
mincost_TMD_l(index)=min(cost_TMD_l{index});
[one mincostScheme_TMD_p(index)]=min(cost_TMD_p{index});
mincost_TMD_p(index)=min(cost_TMD_p{index});
%Find minimum cost scheme for TLCD footprint schemes.
[one mincostScheme_TLCD_c(index)]=min(cost_TLCD_c{index});
mincost_TLCD_c(index)=min(cost_TLCD_c{index});
[one mincostScheme_TLCD_l(index)]=min(cost_TLCD_l{index});
mincost_TLCD_l(index)=min(cost_TLCD_l{index});
[one mincostScheme_TLCD_p(index)]=min(cost_TLCD_p{index});
mincost_TLCD_p(index)=min(cost_TLCD_p{index});
end
end
```

## Appendix H: Total Scheme Costs

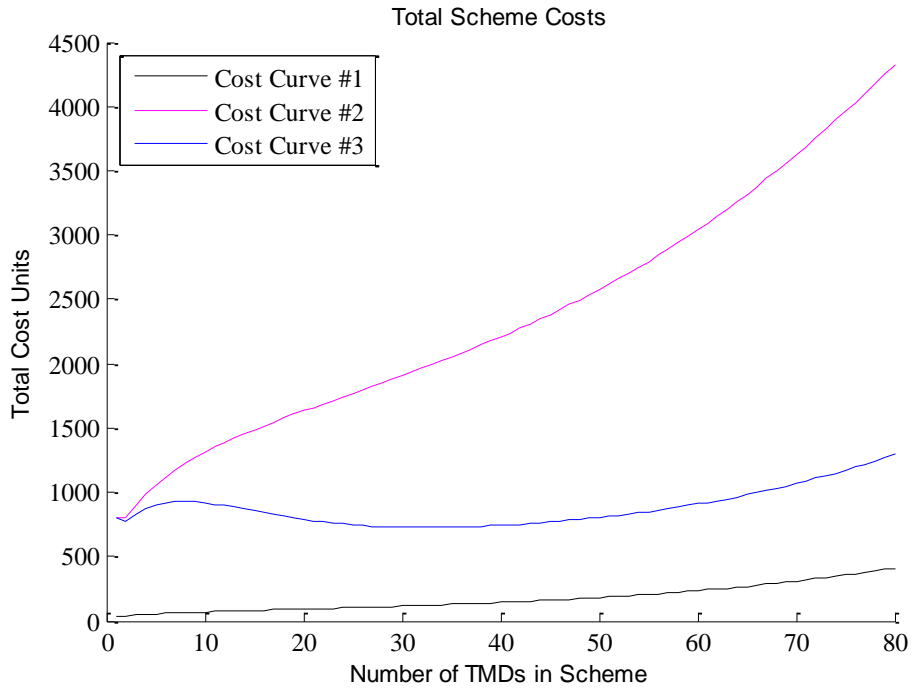


Figure H-1: Total Scheme Costs for 80-story Building with Distributed TMDs

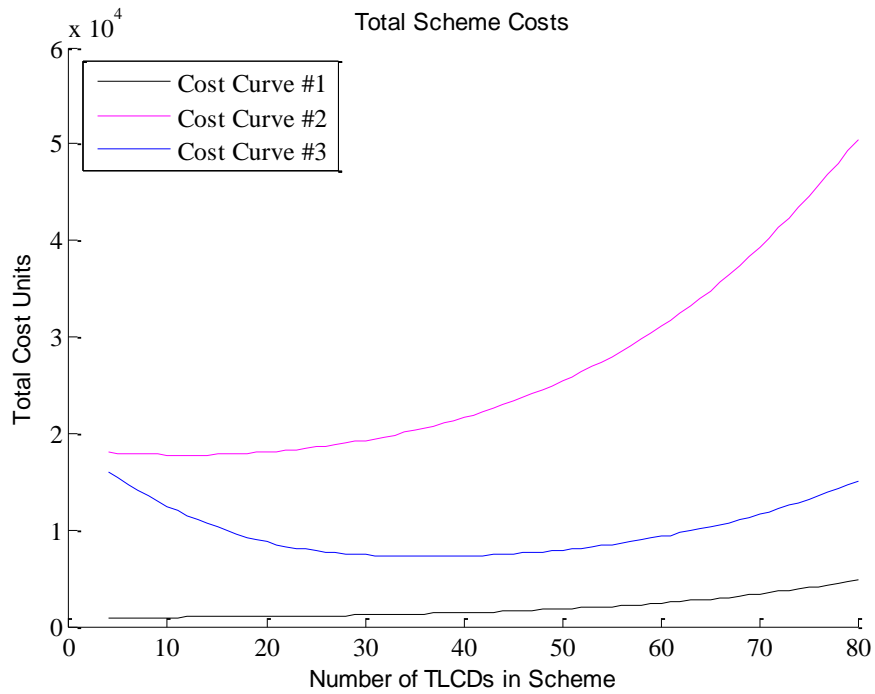
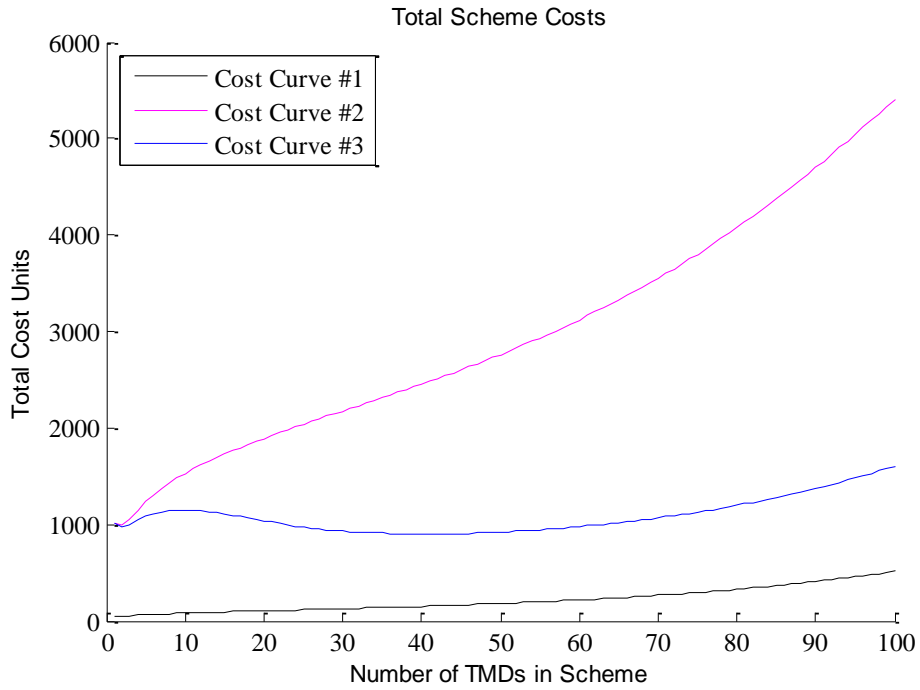
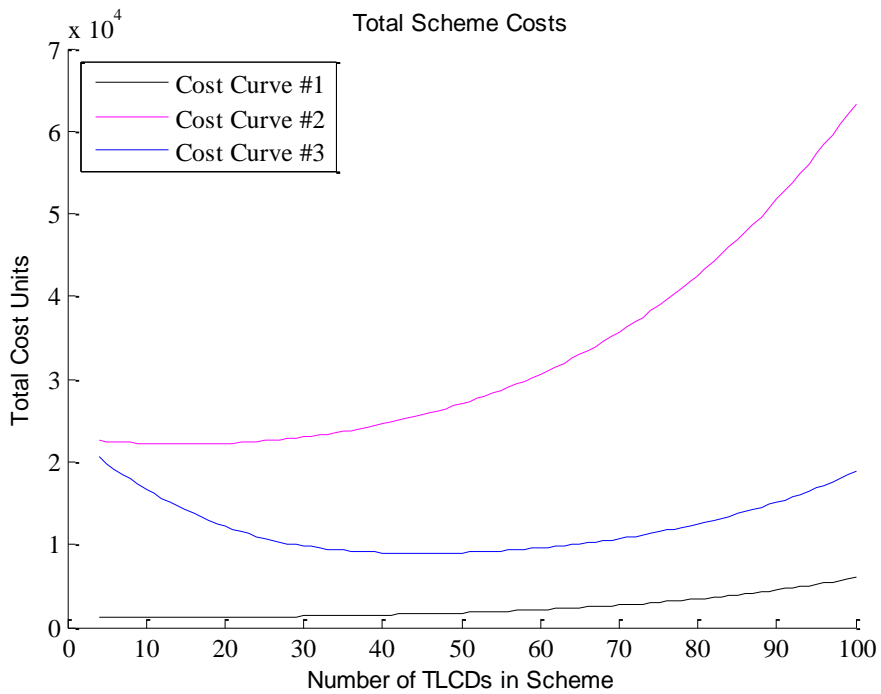


Figure H-2: Total Scheme Costs for 80-story Building with Distributed TLCDs



**Figure H-3: Total Scheme Costs for 100-story Building with Distributed TMDs**



**Figure H-4: Total Scheme Costs for 100-story Building with Distributed TLCDs**

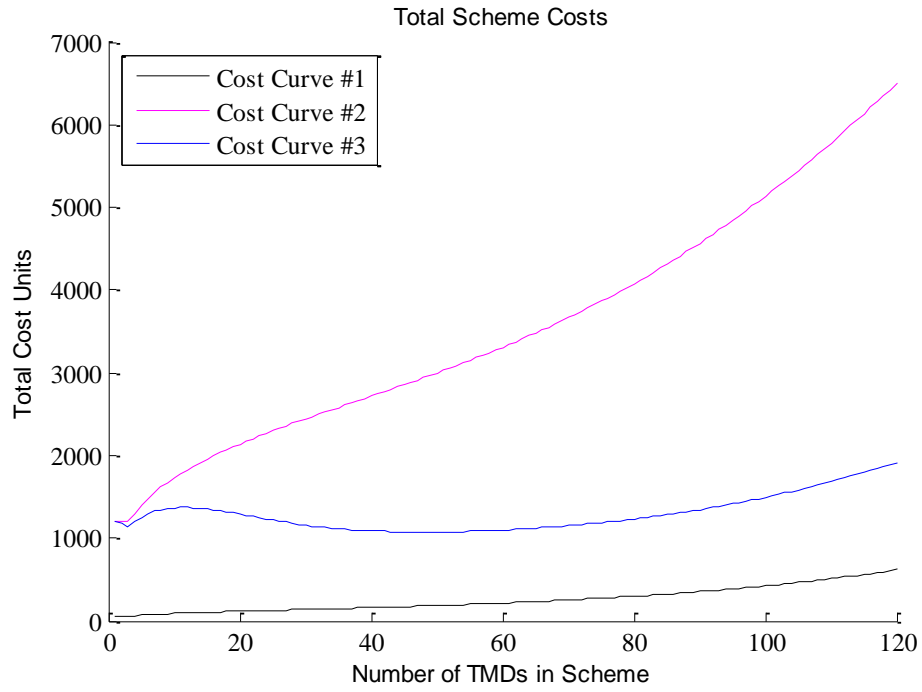


**Figure H-5: Total Scheme Costs for 120-story Building with Distributed TMDs**

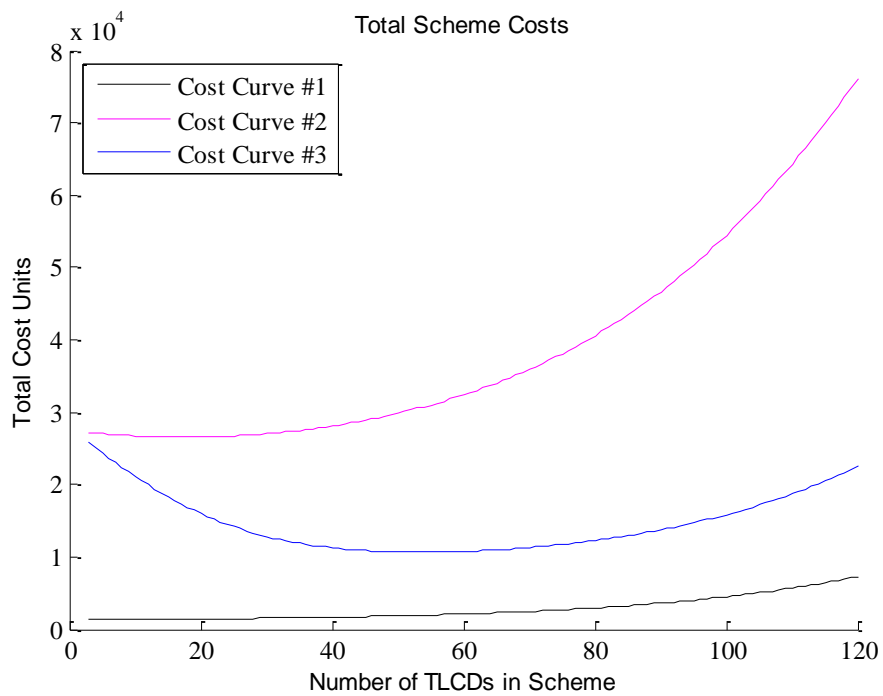


**Figure H-6: Total Scheme Costs for 120-story Building with Distributed TLCDs**



## Works Cited

- Balendra, T., Wang, C. M., & Rakesh, G. (1998). Vibration Control of Tapered Buildings using TLCD. *Journal of Wind Engineering and Industrial Aerodynamics*, 245-257.
- Bergman, L. A., McFarland, D. M., Hall, J. K., Johnson, E. A., & Kareem, A. (1989). Optimal Distribution of Tuned Mass Dampers in Wind-Sensitive Structures. *5th International Conference on Structural Safety and Reliability*, (pp. 95-102). San Francisco.
- Chen, G. (1996). Multi-stage Tuned Mass Damper. *Eleventh World Conference on Earthquake Engineering*. Elsevier Science Ltd.
- Chen, G., & Wu, J. (2001). Optimal Placement of Multiple Tune Mass Dampers for Seismic Structures. *Journal of Structural Engineering*, 1054-1062.
- Colwell, S., & Basu, B. (2006). Investigations on the Performance of a Liquid Column Damper with Different Orifice Diameter Ratios. *Canadian Journal of Civil Engineering*, 588-595.
- Colwell, S., & Basu, B. (2008). Experimental and Theoretical Investigations of Equivalent Viscous Damping of Structures with TLCD for Different Fluids. *Journal of Structural Engineering*, 154-163.
- Connor, J. J., & Laflamme, S. (2014). *Structural Motion Engineering*. Springer-Verlag.  
Manuscript submitted for publication.
- Den Hartog, J. P. (1956). *Mechanical Vibrations*. New York: McGraw-Hill Book Company, Inc.
- Frahm, H. H. (1911). Results of Trials of the Anti-rolling Tanks at Sea. *Journal of the American Society for Naval Engineers*, 571-597.
- Gao, H., Kwok, K. C., & Samali, B. (1997). Optimization of Tuned Liquid Column Dampers. *Engineering Structures*, 476-486.
- Gao, H., Kwok, K. S., & Samali, B. (1999). Characteristics of Multiple Tuned Liquid Column Dampers in Suppressing Structural Vibration. *Engineering Structures*, 316-331.

- Hitchcock, P. A., Kwok, K. C., Watkins, R. D., & Samali, B. (1997). Characteristics of Liquid Column Vibration Absorbers - I. *Engineering Structures*, 126-134.
- Hitchcock, P. A., Kwok, K. C., Watkins, R. D., & Samali, B. (1997). Characteristics of Liquid Column Vibration Absorbers - II. *Engineering Structures*, 135-144.
- Igusa, T., & Xu, K. (1994). Vibration Control Using Multiple Tuned Mass Dampers. *Journal of Sound and Vibration*, 491-503.
- Mayol, E., Samali, B., Kwok, K. C., & Li, J. (2003). Vibration Control of an Experimental Benchmark Model to Earthquake using Liquid Column Vibration Absorbers. *Proceedings of the 10th Asia-Pacific Vibration Conference*, (pp. 451-456). Gold Coast, Australia.
- Moon, K. S. (2005). *Dynamic Interrelationship Between Technology and Architecture in Tall Buildings*. PhD Dissertation, Massachusetts Institute of Technology, Department of Architecture.
- Moon, K. S. (2010). Vertically Distributed Multiple Tuned Mass Dampers in Tall Buildings: Performance Analysis and Preliminary Design. *The Structural Design of Tall and Special Buildings*, 347-366.
- Moon, K. S. (2011). Structural Design of Double Skin Facades as Damping Devices for Tall Buildings. *The Twelfth East Asia-Pacific Conference on Structural Engineering and Construction* (pp. 1351-1358). Procedia Engineering.
- Sakai, F., Takaeda, S., & Tamaki, T. (1989). Tuned Liquid Column Damper - New Type Device for Supression of Building Vibrations. *International Conference on Highrise Buildings*, (pp. 926-931). Nanjing, China.
- Samali, B., Kwok, K. C., & Tapner, D. (1992). Vibration Control of Structures by Tuned Liquid Column Dampers. *IABSE, 14th Congress*, (pp. 461-466).
- Samali, B., Mayol, E., Kwok, K., Hitchcock, P., & Wood, G. (2002). Damping Enhancement of Liquid Column Vibration Absorbers by Use of Orifice Plates. *The 6th Internation Conference on Motion and Vibration Control*, (pp. 271-276). Saitama.

Tsai, H. C., & Lin, G. C. (1993). Optimum tuned-mass dampers for minimizing steady-state response of support-excited and damped systems. *Earthquake Engineering & Structural Dynamics*, 957-973.

Xu, Y. L., Kwok, K. C., & Samali, B. (1992). The Effect of Tuned Mass Dampers and Liquid Dampers on Cross-Wind Response of Tall/Slender Structures. *Journal of Wind Engineering and Industrial Aerodynamics*, 33-54.